Science of the Total Environment 966 (2025) 178677

Contents lists available at ScienceDirect

Science of the Total Environment

journal homepage: www.elsevier.com/locate/scitotenv

# Small-scale fire refugia increase soil bacterial and fungal richness and increase community cohesion nine years after fire

Joseph D. Birch[a,b,*,1,2], James A. Lutz[c,1], Matthew B. Dickinson[d], James Franklin[e], Andrew J. Larson[f,g], Mark E. Swanson[h], Jessica R. Miesel[a,b,2]

[a] *Michigan State University, Department of Plant, Soil and Microbial Sciences, East Lansing, MI 48824, United States of America*
[b] *Program in Ecology and Evolutionary Biology, East Lansing, MI 48824, United States of America*
[c] *Department of Wildland Resources and the Ecology Center, Utah State University, Logan, UT 84321, United States of America*
[d] *USDA Forest Service, Northern Research Station, Delaware, OH, United States of America*
[e] *Independent researcher, Castlegar, British Columbia, V1N 3A2, Canada*
[f] *Department of Forest Management, University of Montana, Missoula, Montana 598212, United States of America*
[g] *Wilderness Institute, University of Montana, Missoula, Montana 59812, United States of America*
[h] *Department of Forest Engineering, Resources, & Management, Oregon State University, Corvallis, OR 97331, United States of America*

## HIGHLIGHTS

- Refugia had notably distinct microbial communities nine years after fire
- Refugia had 19 % greater bacterial and 31 % fungal richness, relative to burned soils
- Burned soils had less robust microbial association networks than refugia
- Fire intensity and severity influenced microbial composition nine years after fire
- Pathogens comprised a larger portion of burned communities relative to refugia

## GRAPHICAL ABSTRACT

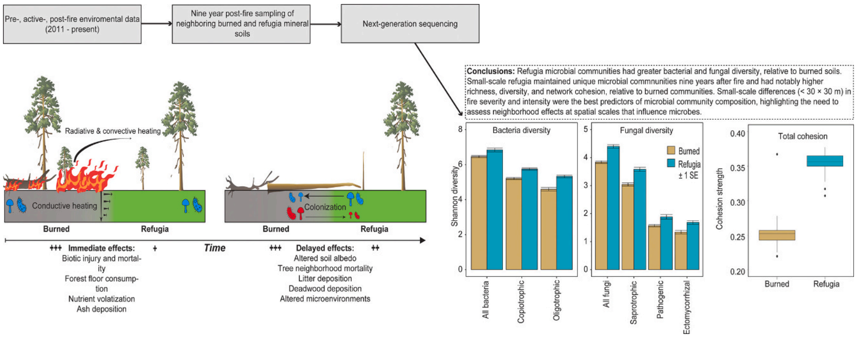

**Conclusions:** Refugia microbial communities had greater bacterial and fungal diversity, relative to burned soils. Small-scale refugia maintained unique microbial commnunities nine years after fire and had notably higher richness, diversity, and network cohesion, relative to burned communities. Small-scale differences (< 30 × 30 m) in fire severity and intensity were the best predictors of microbial community composition, highlighting the need to assess neighborhood effects at spatial scales that influence microbes.

## ARTICLE INFO

Editor: Ewa Korzeniewska

*Keywords:*
Mixed-conifer
Rim fire
Refugia

## ABSTRACT

Small-scale variation in wildfire behavior may cause large differences in belowground bacterial and fungal communities with consequences for belowground microbial diversity, community assembly, and function. Here we combine pre-fire, active-fire, and post-wildfire measurements in a mixed-conifer forest to identify how fine-scale wildfire behavior, unburned refugia, and aboveground forest structure are associated with belowground bacterial and fungal communities nine years after wildfire. We used fine-scale mapping of small (0.9–172.6 $m^2$) refugia to sample soil-associated burned and refugial microbial communities. Richness was higher in refugia for

---

*Abbreviations:* **ASV**, Amplicon sequence variant; **FBAT**, Fire Behavior Assessment Team; **dNBR**, delta normalized burn ratio; **YFDP**, Yosemite Forest Dynamics Plot.

* Corresponding author at: Michigan State University, Department of Plant, Soil and Microbial Sciences, East Lansing, MI, 48824, United States of America.

*E-mail addresses:* jdcooper@uidaho.edu (J.D. Birch), james.lutz@usu.edu (J.A. Lutz), matthew.b.dickinson@usda.gov (M.B. Dickinson), jamesfranklin@ualberta.ca (J. Franklin), a.larson@umontana.edu (A.J. Larson), mark.swanson@oregonstate.edu (M.E. Swanson), jmiesel@uidaho.edu (J.R. Miesel).

[1] These authors contributed equally.

[2] Current address: Forest, Rangeland and Fire Sciences, University of Idaho, Moscow, ID 83844.

https://doi.org/10.1016/j.scitotenv.2025.178677
Received 3 October 2024; Received in revised form 27 January 2025; Accepted 27 January 2025

Yosemite forest dynamics plot
Smithsonian forestGeo
Fire behavior assessment team

bacteria (+19 %) and fungi (+31 %) and in all functional guilds relative to burned soils. Refugial communities had greater proportions of saprotrophic and lower proportions of pathogenic fungi relative to burned soils. Composition differed in burned areas and refugia and was most strongly associated with small-scale fire behavior, aboveground live tree basal area, and tree mortality. Refugial communities had more connected association networks and fewer facilitative interactions relative to burned soils – supporting both the stress-gradient hypothesis and the conclusion that refugial communities may have greater resistance to future disturbance. Small-scale differences in wildfire behavior and effects can have long-term impacts on belowground microbes, highlighting the need to assess neighborhood effects at spatial scales that influence microbes.

## 1. Introduction

Wildfires consume dead and live biomass (e.g., fuel) and release and transport energy via conduction, convection, and radiation (Johnson, 1996). This energy release can alter microbial communities directly through heating-induced damage and death (Dickinson and Johnson, 2004; Rosenberg et al., 1971) or indirectly by altering the physical, chemical, and biotic environment in which the microbes exist (Adkins et al., 2020; Miesel et al., 2015). However, natural spatial variation in plant communities, fuels, weather, and topography may induce 'pyrodiversity' (Jones and Tingley, 2022) – defined as variation in wildfire behavior and effects – which could provide for a gradient of direct impacts on microbes and enable the survival of fire-intolerant microbes (Fox et al., 2022). As well, immediate and delayed vegetation mortality may alter the soil environment, further contributing to microbial community shifts towards more stress-tolerant, pyrophilous, and thus fire adapted communities (Day et al., 2020; Steindorff et al., 2021), which may be long-lasting (Adkins et al., 2022). Therefore, identifying the causes of spatial heterogeneity of wildfire effects is critical for understanding the dynamics after fire of belowground microbial communities and their plant associates.

Consistent with the processes that govern fire extinction (Dickinson et al., 2013; Wilson Jr, 1985). fire that burns under high humidity and/or low wind speed and into discontinuous or moist fuels can create unburned refugia intermixed within a mosaic of burned conditions (Blomdahl et al., 2019; Kolden et al., 2012). Refugia – here defined as areas with intact non-charred organic horizons and unconsumed surface fuels – can vary widely in size and persist through multiple fires (Meddens et al., 2018). Though pyrodiversity and landscape refugia are frequently studied at spatial scales in line with remote sensing data (e.g., 30 × 30 m LANDSAT pixels), this scale may be inadequate for assessing smaller refugia at scales relevant for microbial communities (Birch et al., 2023b; Blomdahl et al., 2019). Small-scale refugia (here defined as smaller than 30 × 30 m), may be important lifeboats for fire-intolerant and late-seral microbial taxa, helping conserve microbial diversity on the landscape (Franklin et al., 2000). Small-scale refugia may be buffered against immediate, direct surface heating from wildfire but still be influenced by delayed fire effects on the landscape including overstory mortality, and changes to infiltration, runoff and erosion, and nutrient cycling (Fig. 1).

As fire intensity (the rate of energy release) and severity (the aboveground and belowground magnitude of organic matter loss; Keeley, 2009) increase, soil fungal and bacterial communities in burned areas generally decline in abundance and richness and become more dissimilar to unburned communities in neighboring forests (Adkins et al., 2020; Whitman et al., 2019). Changes in community composition have been detected within weeks after fire (Bruns et al., 2020; Pulido-Chavez et al., 2021), and persist for decades (Kipfer et al., 2011). However, most studies addressing changes in microbial communities after fire assess fire effects at landscape scales or depend on data from prescribed fire which, by design, does not demonstrate the higher-intensity fire behavior or environmental conditions that occurs during wildfires (Hunter and Robles, 2020). These limitations hamper the ability to understand how fire affects microbial communities at the scale at which fire behavior and effects vary.

Variation in fire behavior may induce differential effects across microbial functional guilds (e.g., symbiotic versus saprotrophic) owing to uneven effects on of living and dead biomass (Birch et al., 2023a), which then determines the habitat and source of nutrients for saprotrophic, symbiotic, and pathogenic microbes. The mortality of large-diameter trees may reduce fine-root availability and thus potential habitat for ectomycorrhizal fungi (Birch et al., 2022; Pulido-Chavez et al., 2021; Taudière et al., 2017) whereas the consumption of organic horizons and soil organic matter may drive shifts in saprotrophic fungi (Beals et al., 2022; Rodriguez-Ramos et al., 2021) by reducing the amount and altering the types of organic material in and above the mineral soil.

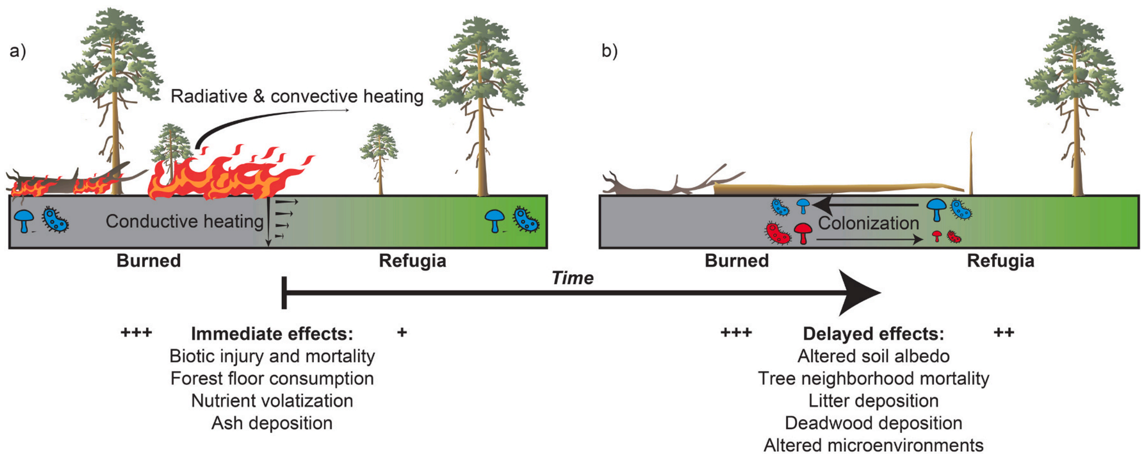

**Fig. 1.** Conceptual diagram of wildfire effects. (a) Burned soils experience immediate direct and indirect effects from wildfire. In contrast, refugia may experience minor heating and minimal immediate impacts from wildfire. (b) Over extended post-fire timeframes there may be bi-directional colonization of soils by bacteria and fungi from communities that experienced differential impacts of wildfire. Long-term delayed effects of wildfire include altered soil albedo, tree mortaliy and root dieback, and differential deposition of deadwood and organic matter onto the forest floor and into the mineral soil.

Conversely, new types and inputs of deadwood - via deposition of fire-killed trees, branches and needles - may increase saprotrophic fungal diversity and abundance over time (Yang et al., 2021). Copiotrophic bacteria (those that favor nutrient-rich environments) often increase in the postfire environment whereas oligotrophic bacteria (those that better tolerate nutrient-poor environments) often decline in abundance (Adkins et al., 2020; Adkins et al., 2022; Pérez-Valera et al., 2019). These changes in microbial community structure may have cascading effects by altering the types, locations, and cycling of nutrients (Kutiel and Naveh, 1987). In turn, changes in the composition and diversity of a single taxon or functional group may have cascading impacts on the entire microbial community through facilitative and competitive interactions (Herren and McMahon, 2018).

Microbial community structure and associations among taxa affect community resistance to potential disturbance such as fire or drought (de Vries et al., 2018; Yang et al., 2022). Inferring the positive or negative associations among microbes can provide insights on which taxa are key to maintaining community structure. In such association networks, taxa are considered ‘nodes’, with associations among taxa inferred as network ‘edges’ between each node (Table 1). Positive correlations between taxa abundances may be inferred as niche overlap or facilitative interactions whereas negative correlations may indicate niche differentiation and competition (Herren and McMahon, 2018). Negative associations between taxa are generally considered to produce networks resilient to disturbances by stabilizing communities and minimizing positive feedback loops (Coyte et al., 2015; Gao et al., 2022); thus, shifts in the abundances of key taxa can alter the ability of the overall microbial community to resist disturbance (Herren and McMahon, 2018), potentially resulting in a fundamental loss of microbial community function (Liu et al., 2022). Because microbial communities may change due to disturbance, the use of comparative microbial association networks may untangle how fire behavior influence vulnerability and resilience to subsequent disturbances.

We investigated the composition of bacterial and fungal communities and their relationships to wildfire behavior, forest composition, mortality, and deadwood deposition in burned soils and neighboring refugia nine years after wildfire in a California mixed-conifer forest. We leveraged unique existing datasets including measurements of active fire behavior, immediate forest change taken within days before and after fire, mapping of small-scale (0.9–172.6 $m^2$) refugia, and long-term forest demography, to address the following research questions:

1) How does microbial diversity vary between burned and refugia soils nine years after fire?
2) How do microbial communities covary with abiotic and biotic environmental neighborhoods after fire?
3) To what extent do network structure and associations differ between burned and refugia communities?

**Table 1**
Description of network characteristics.

| Network term | Description |
|---|---|
| Node | A microbial taxon (agglomerated at the genus level in this study) |
| Edge | An inferred association between nodes (taxa) based on read abundance |
| Average path length | The minimum number of edge steps separating nodes, averaged across all nodes |
| Betweenness | A centrality measure of the number of shortest paths that pass through a node |
| Modularity | A measure of sub-networks (modules) with higher numbers of edges within than between modules (Clauset *et al.*, 2004) |
| Clustering coefficient | A measure of the degree to which nodes are locally connected |
| Largest connected component (LCC) | The largest grouping of nodes that can be traversed through connecting edges. |
| Natural connectivity | A measure of the robustness of networks to deletion of edges (associations) between nodes (Jun *et al.,* 2010) |
| Positive cohesion | The relative strength of positive associations, calculated for each taxa and summed by sample. Bounded between 0 – 1. |
| Negative cohesion | The relative strength of negative associations, calculated for each taxa and summed by sample. Bounded between −1 – 0. |
| Total cohesion | The sum of positive and \|Negative cohesion\|. A measure of network complexity and the strength of associations. |
| Robustness | The proportion of the LCC remaining after progressively removing nodes from the network. |
| Adjusted Rand Index (RDI) | A measure of cluster similarity between two graphs ( Qannari et al., 2014; Hubert and Arabie, 1985). |
| Graphlet Correlation Distance (GCD) | Euclidiean distance between subgraphs. A measure of assessing similarity between graphs (Yaveroğlu et al., 2014) |

## 2. Methods

### 2.1. Study area and pre-fire measurements

The study site was an interior section of the Yosemite Forest Dynamics Plot (YFDP) a 25.6 ha plot established following the protocols of the Smithsonian Forest Global Earth Observatory (ForestGEO, Davies et al., 2021) in Yosemite National Park, California, USA (Lutz et al., 2012). The pre-fire forest community was composed of *Abies concolor* (Gordon & Glendinning) Hildebrand (white fir; 45 % of forest-wide basal area), *Pinus lambertiana* Douglas (sugar pine; 44 % basal area), *Calocedrus decurrens* (Torrey) Florin (incense cedar; 7 % basal area), and *Quercus kelloggii* Newberry (California black oak; 2 % basal area)(Lutz et al., 2012). Prior to modern fire suppression the forest was likely dominated by *P. lambertiana* with smaller cohorts of *Q. kelloggii*, *C. decurrens*, and *A. concolor*. We selected a 2.1 ha sampling area that contained representative tree species, forest structure, topography, and for which we had active-wildfire measurements. All live and dead trees ≥1 cm diameter at breast height (DBH, $n_{2022} = 22{,}189$) were mapped, tagged, identified to species, and annually visited to assess status changes. Additionally, we mapped all deadwood ≥10 cm at its large end that originated from tree boles (n2022 = 13,118, Lutz et al., 2020).

The YFDP spans an elevation of 1773–1911 m with a mean annual temperature of 10.1 °C and mean annual precipitation of 1109 mm, of which 615 mm occurs in the winter (Wang et al., 2016). Most soils are slightly acidic to basic (pH 6.2–7.2) and are within the Alfisol (Palexeralfs), Inceptisol (Dystroxerepts), and Ultisol (Haploxerults) orders with Loamy to Sandy Loam textures. There is no record of management actions taken within the YFDP, though seasonal sheep grazing was present before the inclusion of the land into Yosemite National Park in 1930. The area burned in the human-caused 2013 ‘Rim’ wildfire which burned 104,131 ha in the California Sierra Nevada range (Kane et al., 2015). The YFDP was previously burned by a large fire in 1899; however, the 1986 ‘Bobkitten’ (0.4 ha) and 1984 ‘Quickie’ wildfires (0.4 ha) burned adjacent to the YFDP and may have burned into the edge of the sampling area. Before European colonization and fire suppression, the forest likely burned under frequent, mixed-severity fire with a point fire return interval of 6–34 years (Barth et al., 2015; Safford and Stevens, 2017).

### 2.2. Fire weather, behavior, and measurements after fire

The YFDP burned in a backfiring operation on the 2013 Rim fire. Prior to burning the USDA Fire Behavior Assessment Team (FBAT) established four plots within the YFDP to assess fire behavior using fire-resistant video and sensor arrays (Birch et al., 2023a; Fire Behavior Assessment Team, 2022). Thermocouples provided empirical measures of the rate of spread across the study area (Fire Behavior Assessment Team, 2022). In 2014 all trees and standing dead trees (hereafter snags) were measured for maximum bole char height, bole consumption (%), canopy scorching (%), and mortality. All unburned refugia ≥1 $m^2$ were mapped and delineated by ground crews as described by Blomdahl et al. (2019). Crews used meter tapes and ocular estimation to map refugia polygons in reference to geo-located trees and snags ($n_{2014} = 38{,}664$).

### 2.3. *Forest floor and soil sampling*

In May of 2022, nine years after fire, we collected soil samples across 2.1 ha within the YFDP (Fig. 2).

We established a sampling area consisting of an ordered grid ($n = 60$), randomly placed samples ($n = 26$), and samples randomly placed inside the perimeters of unburned refugia ($n = 35$). We selected this sampling design to enable representative sampling across the study area and refugia while capturing a full range of inter-sample distances so as to assess spatial autocorrelation among samples. At each sampling point, we measured the depths of the organic horizons (litter and duff) to the nearest mm. We used a soil knife (Zenport; Sherwood, Oregon) to sample soil in a 3 × 3 cm area to a depth of 0 — 25 cm, preserving soil from that 25-cm profile. We sanitized the knife using a 10 % bleach solution between each soil sample and froze samples at −20 °C before DNA extraction. Because our study was focused on investigating both direct and indirect effects of fire, we sampled across soil depths that experienced the most intense soil heating (0–10 cm; Brady et al., 2022) and depths that represent indirect fire impacts on roots and organic matter in the nine years after fire (e.g., 0–25 cm; Berndt and Gibbons, 1958; Wasyliw and Karst, 2020). The sampling interval of nine years after fire is within the historic fire return interval (6–34 years) in which microbial communities may be expected to experience subsequent reburns. Four randomly placed samples were in unburned refugia for a total of 78 burned and 43 refugia samples. Refugia samples were located in refugia of 39.1 ± 47.9 $m^2$ SE (range 0.9–172.6 $m^2$). Burned samples were 8.3 ± 5.0 m from the nearest refugia (range 0.3–18.9 m).

### 2.4. *Sample preparation and sequencing*

We freeze-dried soil samples until reaching a stable weight and used MoBio DNeasy PowerSoil Kits (Qiagen, Hilden, Germany) to extract DNA following the manufacturer's instructions. For amplification and sequencing, we targeted the bacterial 16S rRNA region using the 515F and 806R primers (Walters et al., 2016) to target the VF4 region and the fITS7 (Ihrmark et al., 2012) and ITS4 primers for the fungal ITS2 region (Ihrmark et al., 2012; White et al., 1990). Sequencing was conducted at the Utah State University Genomics lab (Utah State University, Logan, UT), with a MiSeq sequencing platform. Eighteen samples (ten burned; eight refugia) had insufficient high-quality DNA and were not successfully sequenced.

### 2.5. *Bioinformatics*

We denoised, quality-checked, and filtered the demultiplexed sequences using the dada2 1.26.0 bioinformatics pipeline (Callahan et al., 2016) for both 16S and ITS sequences which we processed and analyzed separately (Table A.1). We trimmed primers from 16S and ITS sequences using dada2 and cutadapt software (Callahan et al., 2016; Martin,

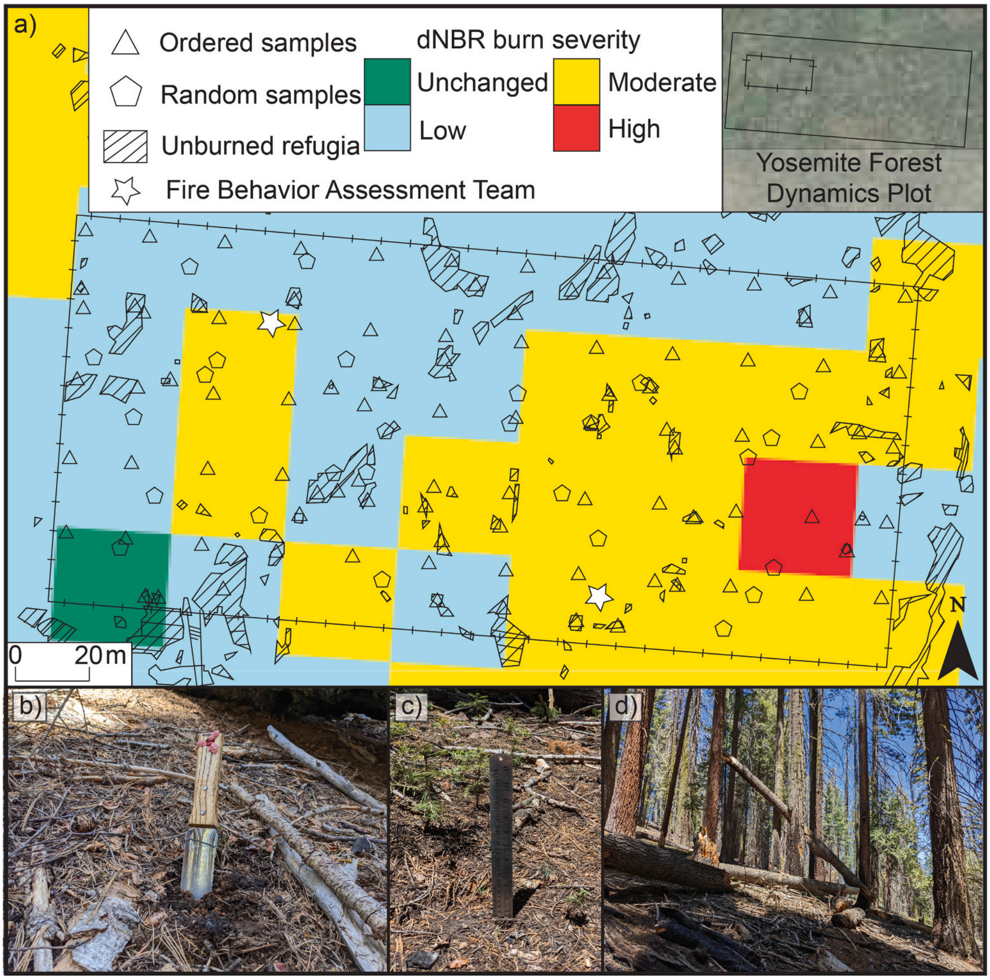

**Fig. 2.** Diagram of sampling area and refugia locations at the Yosemite Forest 2 Dynamics Plot, CA, USA. (a) Map of the sampling locations and delta normalized burn 3 ratio (dNBR) severity. (c:d) Representative photos of the forest floor and sampling area. 4 Photos: Dr. Joseph D. Birch.

2011). We assigned bacterial taxonomy using the SILVA 138.1 database (Callahan et al., 2016; McLaren and Callahan, 2021), with exact species assignments (and fungal taxonomy using the UNITE database (Abarenkov et al., 2023).

We normalized bacterial reads at 12,500 and fungal reads at a 15,000 read cutoff (Fig. A.1) and three bacterial and two fungal samples were below the respective cutoffs. We used non-normalized ASVs for calculating Shannon diversity, richness, and for assessing network associations. We used read-abundance as a proxy for microbial abundance with Bray-Curtis dissimilarity as the frequency of ASVs across samples was positively correlated to read abundance for both bacteria ($R^2 = 0.77$; $P < 0.001$) and fungi ($R^2 = 0.70$; $P < 0.001$).

### 2.5.1. *Functional traits of bacteria and fungi*

To differentiate between oligotrophic and copiotrophic bacteria, we classified all ASVs within Acidobacteriota and Verrucomicrobiota as oligotrophic and ASVs in Actinobacteriota, Bacteroidota, and Firmicutes as copiotrophic (Adkins et al., 2022). To assign functional guilds to fungal ASVs we used the FungalTraits database (Põlme et al., 2020). We assigned guilds at the genus level and grouped similar guilds for analyses (e.g., dung, litter, nectar, pollen, soil, and wood saprotrophs as 'Saprotrophs').

## 2.6. *Characterizing soil nutrients, pH, and moisture*

In 2018 we measured the concentration of mineral soil nutrients (phosphorus, ammonium, nitrate, calcium, iron, potassium, magnesium, manganese, effective cation exchange capacity, base saturation, and sodium) and pH, by sampling soils to 10 cm in a grid across the entire YFDP. We measured soil nutrient concentrations following the analytical methods of Baldeck et al. (2013) and used kriging to interpolate mineral soil pH and nutrients. Prior to interpolating soil nutrients at the YFDP, we normalized each nutrient and plotted semivariograms to assess the spatial autocorrelation of each. We excluded nutrients (ammonium, nitrate, manganese, effective cation exchange capacity, base saturation, and sodium) that were non-normal after transformation and those that were autocorrelated over distances smaller than our sampling distances. We used the 'krige' function in gstat 2–1.0 package (Gräler et al., 2016; Pebesma, 2004) to interpolate the remaining nutrients and then transformed each nutrient to their original units (mg $kg^{-1}$) for analysis (Table A.2). In cases where our models were sensitive to collinearity, we collapsed soil nutrients and pH into principal component scores for each soil sample. After collapsing nutrients, the first (56.4 %) and second (19.8 %) components cumulatively explained 76.2 % of the variation in nutrients (Fig. A.2; Table A.3). Because soil nutrients were collected five years post-fire, we assume that our measurements had captured much of the variability induced by nutrient volatilization from fire and organic inputs, which were concentrated in the immediate post-fire years when tree mortality was at its highest (Furniss et al., 2020). Work by de Vries et al. (2009) suggests that a sampling interval of ≥10 y is needed to detect background changes in soil nutrients (e.g., N, C, base cations) in long-term monitoring plots in European forests. For this study we assume that for the period 2018–2022 that nutrient changes were approximately equivalent and that differences in microsites had equilibrated with time after fire. Comparisons in 2018 of soil nutrients, phosphorous and nitrogen-associated enzymes, and hydraulic connectivity between burned and refugia soils found no significant differences, aside from slightly elevated urease in refugia relative to burned soils (Tamjidi and Lutz, 2020).

Because the study area included vernal streams which may have influenced soil heating and microbial community composition, we calculated the distance to stream and a topographic wetness index as independent variables in our models. To assess if riparian areas influenced the composition of microbial communities, we plotted digitized lidar ground return maps of vernal streams in the YFDP and calculated the linear distance to the nearest 0.1 m between each sampling point and a polyline representing the centroid of the vernal streams (Fig. A.3). This distance to stream (m) metric was used as an independent variable in analyses of microbial composition in combination with a Topographic Wetness Index which was moderately co-linear for our sampling locations (Pearson's correlation = −0.40; Fig. A.3).

## 2.7. *Estimating fireline intensity and burn severity*

To provide context and enable inference with other forests, we assessed wildfire behavior using the active-wildfire and fire effects measurements of the FBAT in and around the immediate (~100 m) sampling area. A Fire Behavior Analyst (National Wildfire Coordinating Group, 2024) watched each of the four videos of the wildfire in the YFDP (Reiner et al., 2021) and recorded the mean and ranges of fire behavior (e.g., flame lengths and the heights, rates of spread, and direction of travel of fire). We calculated woody and herbacous surface fuel moistures at the time of fire using Fire Family Plus 5 (Bradshaw and McCormick, 2000) parameterized with interpolated hourly weather data (Table A.4). We used thermocouples and fire video (Fig. A.4) to assess the rate of spread (m $sec^{-1}$) of the flaming front.

We estimated fireline intensity (kW $m^{-1}$) using post-fire bole char heights collected across the YFDP. Fireline intensity is a measure of the energy release per unit space along the flaming front of a wildfire and is closely related to flame height, length, and fire severity (Alexander and Cruz, 2012; Byram, 1959). Because estimating fireline intensity from bole char heights may be biased in wind-driven fires (Gill, 1974), we retrieved hourly weather from a station located 0.5 km south of the YFDP (National Weather Service, 2023) to parameterize the program WindNinja 3.9.0 (Rocky Mountain Research Station, Missoula, MT) to model wind-speeds. We downscaled 10 m winds from WindNinja to mid-flame windspeeds using the FirebehavioR 0.1.2 R package and using pre-fire fuel height measurements (Birch et al., 2023a; Ziegler et al., 2019). Our estimates of wind speeds and four FBAT videos of fire behavior in the YFDP indicated light 0–5 km $h^{-1}$ winds, which justified using bole char heights to estimate fireline intensity.

To estimate fireline intensity we used an equation (Eqtn. 1) which related bole char height to fireline intensity and was developed in *Pinus banksiana* Lambert (jack pine) stands (Weber et al., 1987). For the 34,160 points where we had post-fire measurements of maximum bole char height, we calculated intensity as:

$$Intensity\ \left(kW\ m^{-1}\right) = exp\left(2.64 + \frac{Height\ of\ char\ (m)}{0.36}\right) \quad (1)$$

After interpolated intensity from the values at all 34,160 trees and snags, Prior to interpolation we first normalized all intensity values using 'powerTransform' function in the car 3.1–2 package (Fox and Weisberg, 2018) and confirmed normality of the transformed values by plotting histograms and using a Shapiro-Wilk test. We originally attempted to krige between all point estimates of intensity but found that R was incapable of processing such a large dataset, even when utilizing a high performance computing cluster (HPCC; Michigan State University). To reduce the complexity of the dataset, we generated 2.5 × 2.5 m pixels across the YFDP, and averaged the intensity values of all points in each pixel. After removing pixels with no trees, we had 18,692 pixels, and we used the centroids of each pixel as estimates of mean intensity. We krigged the normalized intensity after assessing that autocorrelation range was greater than the mean distance between trees. After interpolation, we back-transformed normalized intensity values to enable interpretation in the original units (kW $m^{-1}$). We adjusted all refugia intensity values to '0' to represent an unburned state. Intensity values represented a relative comparison of fire intensities across the study area with individual measurements skewed upwards by isolated torching of snags (therefore representing the uppermost range of intensities expected during a surface fire (Van Wagner, 1983).

To identify how burn severity is associated with microbial community composition we assessed both a remote sensing offset-adjusted delta normalized burned ratio (dNBR, Key and Benson, 2006) using categorical severity thresholds established by Miller and Thode (Miller and Thode, 2007) and soil burn severity (SBS) from the Burned Area Emergency Response (Burned Area Emergency Response, 2013). The dNBR assesses changes in the surface reflectance of predominantly overstory vegetation at scales of 30 × 30 m, from image pairs taken before and one-year post-fire (Key and Benson, 2006). The burned area emergency response soil burn severity is an immediate (days to weeks) post-fire data product developed for each fire and validated against remote-sensing reflectance measures to extrapolate categorical (e.g., ‘very low, ‘low, “moderate”, and “high”) measures of soil burn severity (Parsons et al., 2010). To estimate the consumption of litter and duff across the YFDP we compared paired pre-fire (2011) and post-fire (2014) litter and duff depth measurements ($n = 1120$) taken along the boundaries of the YFDP (Cansler et al., 2019) to identify the relative (%) consumption due to wildfire.

### 2.8. Statistical analyses

We conducted all statistical analysis using the R 4.2.1 statistical software with the graphical user interface R Studio, 2023.06.02 (R Core Team, 2022; R Studio Team, 2023). We analyzed our results using the phyloseq 1.42.0, vegan 2.6–4, and phyloseqGraphTest 0.1.0 R packages (Fukuyama, 2023; McMurdie and Holmes, 2013; Oksanen et al., 2023). We visualized our results using ggplot2 3.4.4, ggpubr 0.6.0, and igraph 1.5.1 R packages (Csárdi and Nepusz, 2006; Csárdi et al., 2024; Kassambara, 2023; Wickham, 2016) and produced maps in ArcMap 10.8.1 (ESRI, Redlands, California).

To identify the direct and indirect influences of fire and the environment on microbial communities' richness and composition we identified a priori explanatory variables including sample type (burned or refugia), fire behavior (fireline intensity), fire effects (dNBR, SBS burn severity, mortality 2014–2021), soil nutrients (Al, Ca, Fe, pH, K, Mg, P), topography (elevation, topographic wetness, distance to stream), and abundance of live trees and dead biomass (litter and duff depth, deadwood biomass; Fig. 3). We used an analysis of variance (ANOVA) in base R to assess if environmental variables differed between burned and refugia samples and verified assumptions of normality and heteroscedasticity using a Shapiro-Wilks and Bartlett test, respectively (R Core Team, 2022). We tested litter and duff depths using data from all samples, including those not successfully sequenced.

#### 2.8.1. Neighborhood analysis of live trees, mortality, and deadwood biomass

To identify the potential spatial neighborhood which may influence belowground communities, we tested for spatial autocorrelation among

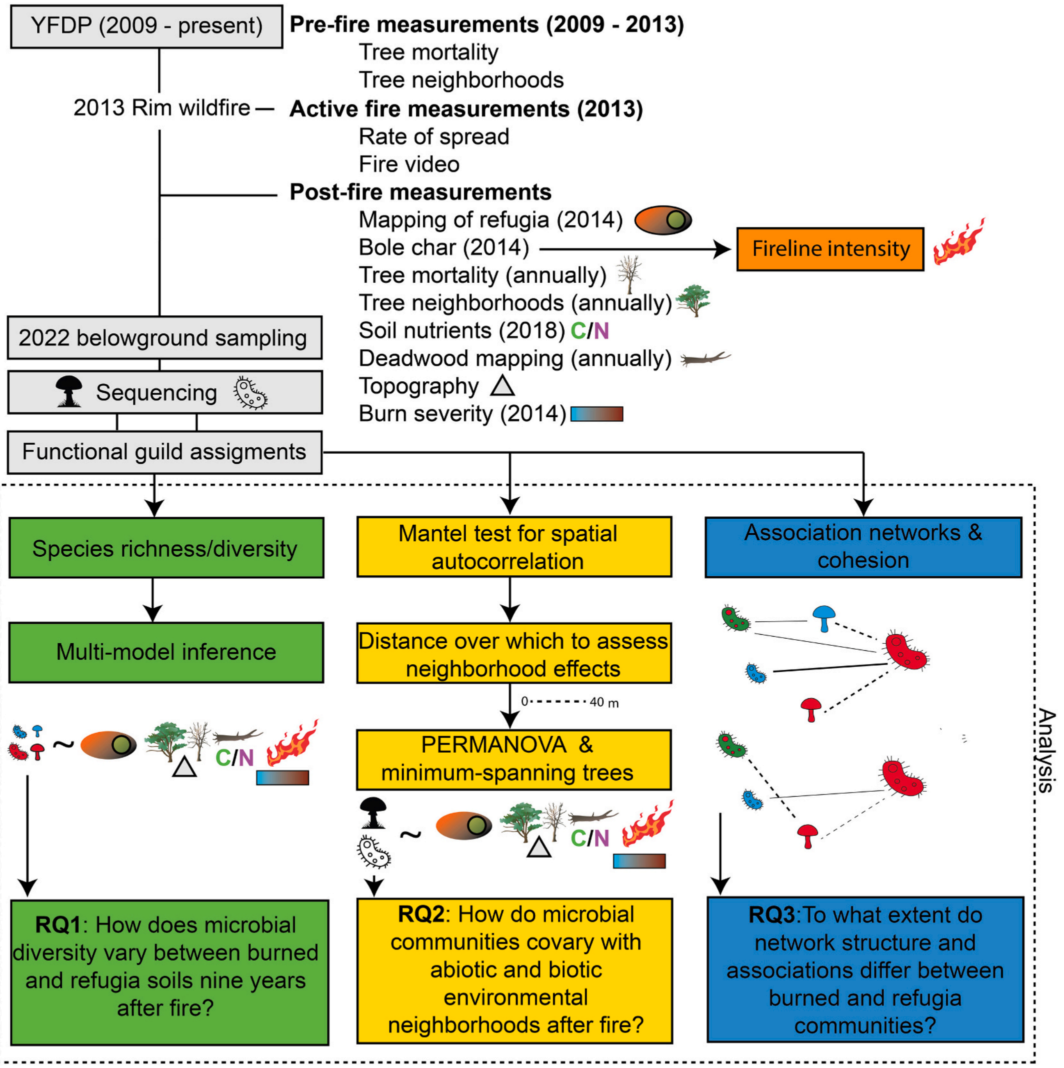

**Fig. 3.** Diagram of the data and analyses used to address our research questions at the Yosemite Forest Dynamics Plot (YFDP), CA, USA.

bacterial and fungal communities using a Mantel test in the vegan 2.6–4 R package (Oksanen et al., 2023). We tested burned and refugia communities separately and minimized the risk of false positives by inversely weighted all (dividing) neighborhood values by the distance of each to the sampling point. We tested pairwise-Euclidean distances and Bray-Curtis dissimilarity and found spatial autocorrelation (0–40.0 m) for burned fungi and no patterns of autocorrelation for all bacterial and fungal refugia communities (Fig. A.5). We then used the maximum spatial range of burned fungal communities over which to summarize the scales at which the aboveground forest may influence belowground communities.

We summed the basal area for all living trees in 2022 in a 40 m buffer of each sampling location and divided the basal area by the distance between the sampling location and the tree stem (Eqtn. 2;).

$$Weighted\ Basal\ Area_{Live\ trees} = \sum \frac{Basal\ Area\ (m^2)}{Distance\ from\ sampling\ location\ (m)} \tag{2}$$

To assess the influence of trees that died after the wildfire, we used similar methods as for live trees, with the modification that we weighted snag basal area by the number of years the tree had been dead to account for a greater period in which they had influenced microbial communities (Eqtn. 3).

$$Weighted\ Basal\ Area_{Snag} = \sum \frac{Basal\ Area\ (m2)}{Distance\ (m)} {*}Time\ since\ death \tag{3}$$

To assess the influence of deadwood on microbial communities, we calculated the mass (Mg) of all mapped deadwood following Lutz et al. (2020) using the species and decay-class specific coefficients of Harmon et al. (2008) and Cousins et al. (2015). We first calculated a 40 m radius around each sampling point and assessed the overlap for each deadwood polygon and the radial buffer. We adjusted our biomass estimates for each piece of deadwood by the percentage of the polygon overlapping the 40 m buffer and weighted biomass by the distance between the sampling location and the centroid of the intersecting deadwood polygon.

### 2.8.2. *Assessing the environmental influences on microbial richness*

To calculate Shannon's diversity and richness we used phyloseq 1.38.0, on un-rarefied community data (McMurdie and Holmes, 2013). We calculated beta diversity following Whittaker (1960) with separate calculations for burned and refugia samples and gamma diversity derived from the total richness of both burned and refugia samples within the YFDP. To test which environmental factors were associated with microbial richness, we used a multi-model inference (MMI) approach using the MuMIn 1.4.75 package (Bartoń, 2022). A MMI calculates all possible combinations of models, based on a priori hypothesis, and weights models according to AICc, with a global model produced by averaging the top-ranking models (ΔAICc from the best model), with models ranked by the explanatory power. We chose a ΔAICc threshold of $<3.0$, indicative of highly skilled models. Individual variables were assigned a relative variable importance (RVI), with an RVI $\geq 0.5$ considered an 'important' variable in explaining microbial richness. Because the MMI is sensitive to multi-collinearity, we calculated a variable inflation score (VIF), collapsed soil nutrients into two principal coordinates and removed elevation to reduce the VIF $< 3$ for all variables.

### 2.8.3. *Assessing drivers of compositional differences*

To visualize composition differences between burned and refugia microbial communities we conducted a minimum spanning tree analysis in the phyloseqGraphTest 0.1.0 R package (Fukuyama, 2023) with 999 permutations based on Bray-Curtis dissimilarity and the grouping factor selected as sample type. To determine how microbial communities covary with post-fire abiotic and biotic environmental neighborhoods we used Bray-Curtis community dissimilarity of bacterial and fungal communities as a dependent variable in a permutational analysis of variance (PERMANOVA) in vegan 2.6–4 (Oksanen et al., 2023). We used as explanatory variables both the categorical burned/refugia status as well as the estimated fireline intensity because intensity provides a continuous estimate of direct fire effects. Other explanatory variables included measures of soil nutrients, topography, fire severity, neighborhoods for live trees, snags, and deadwood. Prior to using a PERMANOVA, we verified assumptions of homogeneity of multivariate dispersions by calculating beta dispersion and using a Tukey Honest Significant Differences test to verify that burned and refugia samples were not different ($P > 0.05$).

### 2.8.4. *Network associations & inferred assembly processes*

To assess the network associations between ASVs, we analyzed unrarefied bacterial and fungal communities agglomerated at the genus level using a Pearson correlation analysis and the NetCoMi 1.1.0 R Package (Peschel, 2023; Peschel et al., 2020). We agglomerated communities at the genus level to avoid inferring intraspecific association patterns in ASVs that can overrepresent diversity by 30–110 % (Glassman and Martiny, 2018). Because we had an unbalanced design, we down-selected a random subsample of burned samples to ensure equal representation between groups ($n_{total} = 72$). Prior to agglomeration, we separately filtered bacterial and fungal genera to only those that had $\geq$ median read abundance and were present in $\geq 5$ samples (14 %). We used a centered-log-ratio transformation of read counts, an unsigned transformation to weight negative and positive associations equally, maintained edges with a correlation $\geq 0.5$, and used a multiplicative simple replacement for zeros. To identify clusters in the network, we used a fast-greedy clustering algorithm implemented using the iGraph 1.5.1 (Csárdi et al., 2024) package with hubs identified using degree and eigenvector centrality, with a fitted log-normal distribution and hubs as those with in the upper Q4 quantile (Appendix B). We calculated topological properties relating to network stability (Table 1) and calculated the positive and negative cohesion of each network using a null-model taxa-shuffle and analytical code of Herren and McMahon (Herren and McMahon, 2018) where:

$$Cohesion_{Positive} = \sum_{i=1}^{n} Relative\ abundance_{i,j} \times positive\ connectedness_i$$

$$Cohesion_{Negative} = \sum_{i=1}^{n} Relative\ abundance_{i,j} \times negative\ connectedness_i$$

And

$$Cohesion_{Total} = \left|Cohesion_{Negative}\right| + Cohesion_{Positive}$$

Cohesion represents a weighted measure, per sample, of the mean sign and strength of associations among taxa, weighted by the relative abundance of each taxon. Negative cohesion is generally associated with more stable microbial communities whereas positive cohesion can indicate vulnerability to disturbance (Coyte et al., 2015; de Vries et al., 2018; Hernandez et al., 2021). To assess if network topologies differed between sample types, we calculated the adjusted Rand Index (RDI) and graphlet correlation distance (GCD) using the NetCoMi 1.1.0 R Package and 1000 permutations against a null model of no difference (Peschel, 2023). The RDI is bounded between −1 and 1, where 1 indicates complete agreement between network clusters and 0 indicates independence between graphs (Hubert and Arabie, 1985; Qannari et al., 2014). The GCD is the Euclidean distance between the upper triangle of correlation matrices derived from network's nodes within subgraphs (e.g., 'graphlets') and provides a metric for robustly comparing network topology (Hočevar and Demšar, 2016; Yaveroğlu et al., 2014).

## 3. Results

### 3.1. Fire behavior and effects

The study area burned between 7:39 UTC Sept 1 and 18:30 Sept 2 2013 as part of a backfiring operation originating 0.5 km to the south. Surface fuel moistures were low ($\leq$15 %; Table A.4) with relative humidity of 36–74 % (mean 56 ± 1.6 SE %) and air temperatures ranged from 15.2 to 25.3 °C (mean 19.3 ± 0.4 °C SE). Fire behavior was low to moderate with backing and flanking fire behavior across the study site (Fig. 4, Fig. A.4). Flame lengths ranged from 0.5 to 10.0 m, with a mean flame length of 0.6 m and only 18.5 % of bole char heights matching or exceeding half of their respective bole height (Fig. A.5). Estimated fireline intensity had a median of 2906 ± 7299 kW m$^{-1}$ at burned sampling locations. Maximum bole char height on the nearest tree were 1.7 m greater for burned samples (mean height = 2.7 ± 0.3) than for refugia samples (Fig. 4).

Burn severity, as assessed by the delta normalized burn ratio (dNBR) at a 30 × 30 m scale, averaged 176 ± 7 SE, and did not differ ($F_{100}$ = 1.27, $P$ = 0.262) between burned and refugia samples. Consumption was high for litter (83 % ± 0.8 % SE) and duff (93 % ± 0.9 %), the fuels most proximate to the mineral soil. In 2022, neither the depth of litter nor duff differed between burned and refugia samples, nor did elevation or soil nutrients, as measured in 2018 (Table A.5). Tree mortality generally followed expectations for the mixed-conifer zone of the Sierra Nevada – large-diameter trees mostly survived the immediate fire effects whereas small-diameter trees experienced >90 % mortality as assessed in 2014. Fire-weakened trees were often killed by bark beetles in the years following the fire (Furniss et al., 2020). Tree mortality after fire (2013−2021) ranged from basal area losses of 14.6–50.8 m$^2$ ha$^{-1}$ across the sampling area and did not differ between burned and refugia areas (Table A.5).

### 3.2. Environmental drivers of microbial richness

After merging filtered, non-chimeric sequences, there were 4,478,039 bacterial and 3,721,575 fungal reads and read number and length did not vary between burned and refugia samples ($P$ > 0.05). After rarefaction, there were 12,932 bacterial amplicon sequence variants (ASVs; 98 samples) and 4596 fungal ASVs (100 samples). Proportional read abundances were similar at the phylum and family level between burned and refugia communities. For bacteria, Micrococcaceae was the most read-abundant family, followed by Solirubrobacteraceae and Xanthobacteraceae (Table A.6). For fungi, the most read-abundant families were Melanommataceae, Aspergillaceae, and Cylindrosympodiaceae (Table A.6). The most read-abundant bacterial genera across all samples included *Pseudarthrobacter*, *Conexibacter*, and *Gemmatimonas* (Appendix C), whereas *Herpotrichia*, *Penicillium*, and *Cylindrosympodium* were the most read-abundant fungi (Appendix C).

Across all burned and refugia samples, we identified 1567 oligotrophic (8.2 % of reads) and 3841 copiotrophic ASVs (49.6 % of reads). Refugia communities had 178 more oligotrophic (576 vs. 398 ASVs) and

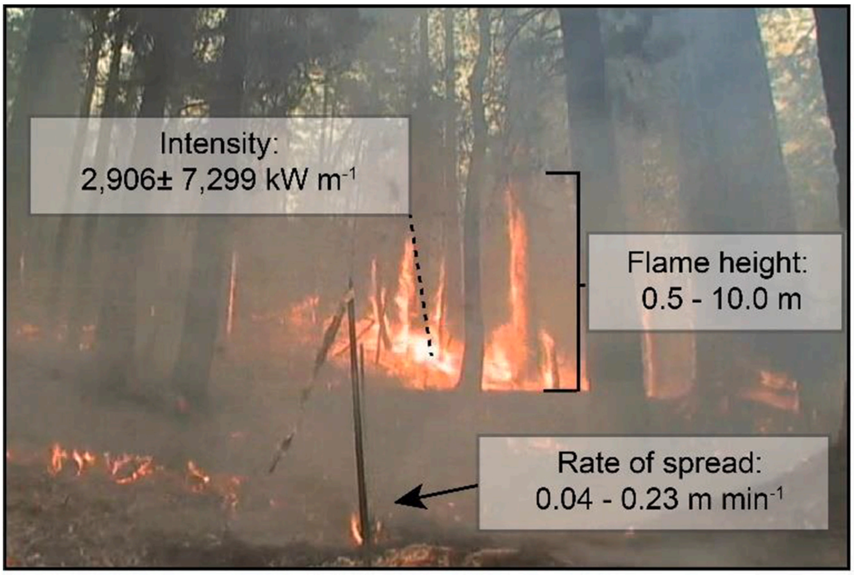

| Fire effects | Burned | Refugia |
|---|---|---|
| Nearest live tree (m) pre-fire | 2.0 ± 0.1$^{a}$ | 2.3 ± 0.2$^{a}$ |
| Nearest live tree (m) in 2022 | 5.5 ± 0.4$^{a}$ | 3.7 ± 0.3$^{b}$ |
| Live overstory (m$^2$) in 2022 | 19.6 ± 0.8$^{a}$ | 22.4 ± 1.0$^{b}$ |
| Max char (m) on nearest tree in 2014 | 2.7 ± 0.3$^{a}$ | 1.0 ± 0.2$^{b}$ |
| Canopy scorch (%) on nearest tree in 2014 | 74 ± 5$^{a}$ | 60 ± 8$^{a}$ |
| Overstory mortality (m$^2$) (2013 – 2021) | 16.0 ± 0.5$^{a}$ | 15.1 ± 0.7$^{a}$ |
| Nearest snag (m) before fire | 1.9 ± 0.1$^{a}$ | 2.7 ± 0.2$^{b}$ |
| Nearest snag (m) in 2022 | 2.8 ± 0.2$^{a}$ | 3.3 ± 0.2$^{a}$ |
| Nearest deadwood pre-fire | 6.6 ± 0.6$^{a}$ | 6.0 ± 0.6$^{a}$ |
| Nearest deadwood in 2022 | 6.3 ± 0.5$^{a}$ | 7.8 ± 0.7$^{a}$ |

**Fig. 4.** Fire behavior and effects with annotated screen-capture of fire behavior from Fire Behavior Assessment Team video in the Yosemite Forest Dynamics Plot, CA, USA. Mean values ±1 SE for fire effects and forest structure for burned and refugia samples. Different lowercase letters indicate significant ($P$ < 0.05) differences between samples assessed using an Analysis of Variance (ANOVA).

256 more copiotrophic bacteria (1510 vs 1254) and a greater oligotrophic to copiotrophic ratio (0.2 vs 0.15) relative to burned samples (Table A.7). We identified 197 ectomycorrhizal fungal ASVs (4.7 % of all reads), 1165 saprotrophic fungal ASVs (34.2 % of all reads), and 187 pathogenic fungal ASVs (19.0 % of reads), with 1710 low read abundance ASVs (19.8 % of reads) having insufficient information for a functional guild classification. Burned and refugia soils shared 11,153 bacterial ASVs (89 % of all ASVs) and 3199 fungal ASVs (69 %) which cumulatively represented 98.9 % and 97.3 % of all reads, respectively (Table A.8). Refugia communities had a 10 % higher proportional read abundance for saprotrophic fungi (40.8 ± 2.0 SE %) relative to burned samples (30.8 ± 1.2 %; $P < 0.001$). In contrast, burned communities had 7 % greater proportional read abundance of pathogenic fungi in burned (21.3 ± 1.6 %) relative to refugia samples (14.6 ± 1.6 %; $P = 0.001$; Table A.9).

There were significant, but slight (3–4 %) differences between refugia and burned communities in the proportional read abundance of copiotrophic and oligotrophic guilds, and no difference for ectomycorrhizal fungi (Table A.9). Despite the high overlap in ASVs, burned and refugia samples were compositionally dissimilar, driven by differential abundance of taxa (Fig. 5). Minimum-spanning trees showed that on average, communities were most similar to other communities from the same sample type (e.g., refugia – refugia; Fig. 5).

Both bacterial and fungal richness and Shannon diversity were elevated in refugia, relative to burned samples (Fig. 6a). Shannon's diversity and community richness were greater in refugia samples for all functional guilds ($P < 0.05$; Table A.7). Whittaker's beta diversity for bacteria was 3.51 in burned samples and 2.96 in refugia samples (Table A.7) whereas fungal beta diversity was 8.26 in burned samples and 6.28 in refugia samples. Our multi-model inference approach identified the most important (relative variable importance [RVI] ≥ 0.5) variables associated with richness of the bacterial and fungal communities. The global model, averaged across the top performing models ($\Delta$AICc ≤0.3; Appendix C), indicated that bacterial richness was greater in refugia (RVI = 1.00; Fig. 6), greater with increasing distance-weighted basal area of live trees (RVI = 0.91), greater with greater litter depth (RVI = 0.74), and declined with increasing fireline intensity (hereafter 'intensity'; RVI = 0.55). Copiotrophic bacterial richness was greater in refugia (RVI = 1.00, Fig. 6d), greater with higher litter depth (RVI = 1.00), and declined with increasing intensity (RVI = 0.81). Oligotrophic bacterial richness was greater in refugia (RVI = 1.00, Fig. 6e), greater with higher litter depth (RVI = 1.00), greater with increasing distance-weighted basal area of live trees (RIV =0.97), and declined with increasing intensity (RVI = 0.64). Total fungal richness was elevated in refugia (RVI = 1.00; Fig. 6f) and was elevated with greater distance-weighted basal area of live trees (RVI = 1.00). Saprotrophic fungal richness was elevated in refugia (RVI = 1.00) and was elevated with greater distance-weighted basal area of live trees (RVI = 1.00), but was negatively related to duff depth (RVI = 0.56; Fig. 6g). Pathogenic fungal richness was elevated in refugia (RVI = 0.72; Fig. 6h) and was elevated

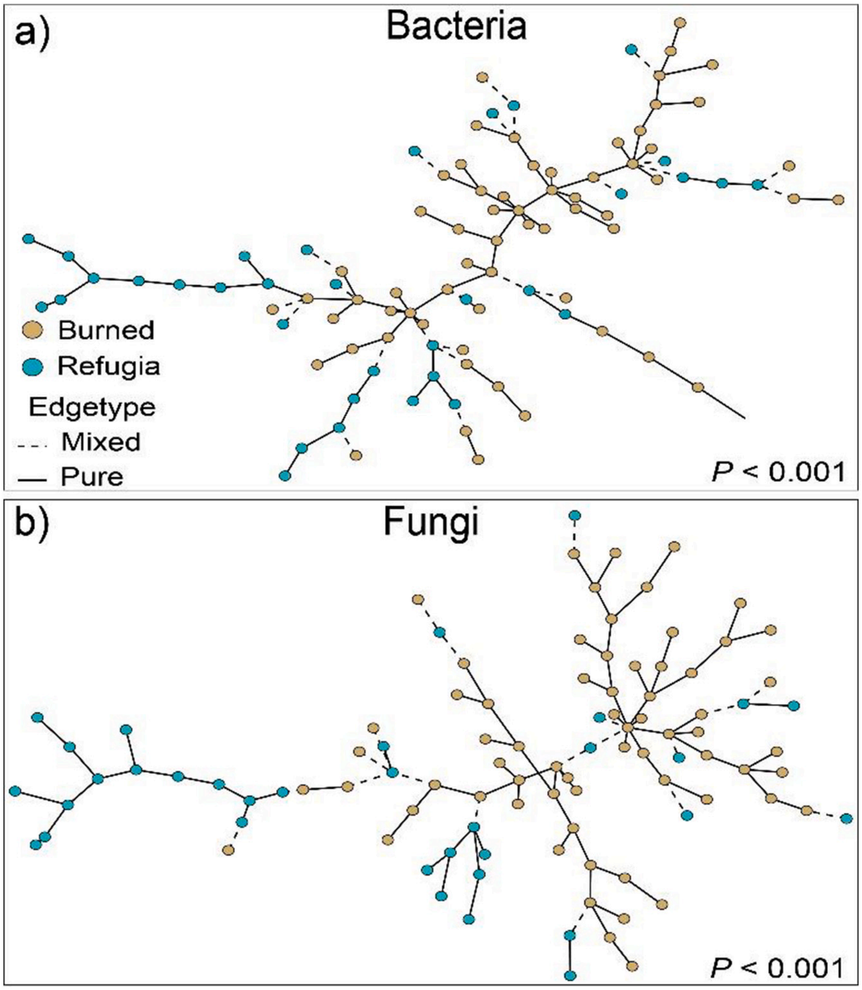

**Fig. 5.** Minimum-spanning trees for bacterial and fungal communities for (a) bacterial and (b) fungal communities at the Yosemite Forest Dynamics Plot, CA, USA. Edges connect most-similar samples of the same (pure; e.g., refugia – refugia) or different types (mixed; e.g., refugia – burned). Both burned and refugia bacterial and fungal communities had more pure edges than expected by chance ($P < 0.001$).

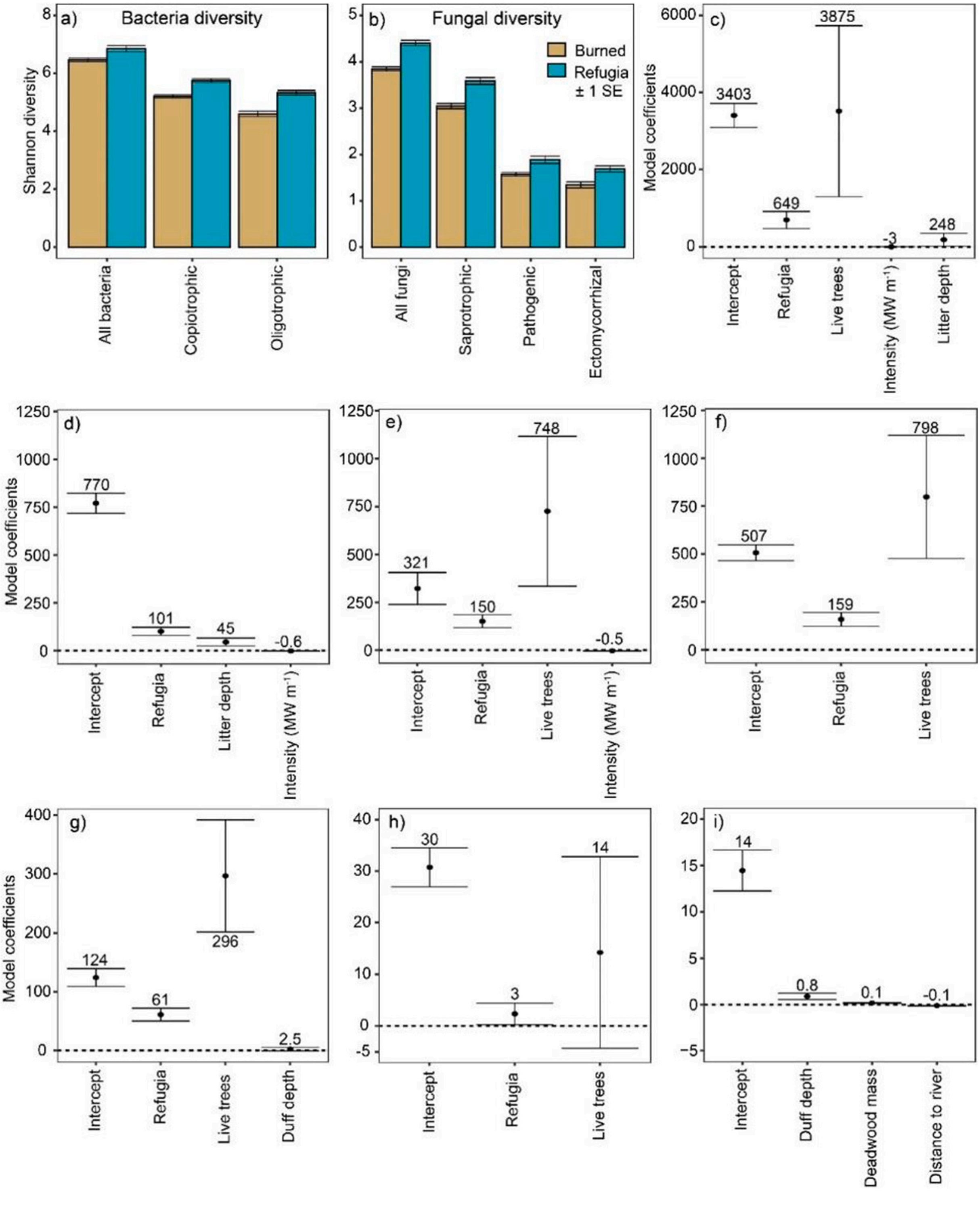

**Fig. 6.** Shannon diversity and coefficients for richness of burned and refugia microbial communities at the Yosemite Forest Dynamics Plot, CA, USA. Shannon diversity for bacterial (a) and fungi (b) functional guilds were different ($P < 0.001$) between burned and refugia communities for all guilds. The estimated coefficient values ±1 SE for all variables with an relative variable importance ≥0.5 for (c) all bacteria, (d) copiotrophic bacteria, (e) oligotrophic bacteria, (f) all fungi, (g), saprotrophic fungi (h) pathogenic fungi, and (i) ectomycorrhizal fungi from globally averaged models. Units: Live trees (m2 m-2), Intensity (MW m-1), litter depth (cm), duff depth (cm), deadwood mass (Mg m-2), distance to stream (m).

with greater distance-weighted basal area of live trees (RVI = 0.50). Ectomycorrhizal fungal richness was elevated with greater abundance of deadwood (RVI = 1.00, Fig. 6i) and with greater duff depth (RVI = 1.00) but was negatively associated with proximity to vernal streams (RVI = 1.00).

PERMANOVAs of microbial composition identified functional-guild-specific environmental covariates of composition with sample type (e.g., burned or refugia) and soil iron content being significant across most functional guilds (Table 2). Estimated fireline intensity was a significant predictor for all functional guilds save ectomycorrhizal fungi whereas soil pH was significant for all guilds except pathogenic fungi. Remote-sensing derived burn severity metrics were significant predictors for

**Table 2**

PERMANOVA output for bacteria and fungal communities in the Yosemite Forest Dynamics Plot, CA, USA. $R^2$ values are provided with asterisks denoting significance as: '*' = $P < 0.05$, '**' = $P \leq 0.01$, and '***' = $P \leq 0.001$. Non-significant variables are denoted as 'ns'.

| Category | Variable | All Bacteria | Copiotrophic bacteria | Oligotrophic bacteria | All fungi | Ectomycorrhizal fungi | Saprotrophic fungi | Pathogenic fungi |
|---|---|---|---|---|---|---|---|---|
| Fire effects | Burned or refugia | 0.053 (***) | 0.059 (***) | 0.040 (***) | 0.047 (***) | 0.013 (*) | 0.052 (***) | 0.044 (***) |
| | Delta normalized burn ratio (dNBR) | ns | ns | ns | ns | 0.013 (*) | ns | ns |
| | Soil burn severity (SBS) category | ns | 0.016 (*) | ns | ns | ns | ns | ns |
| Fire behavior | Fireline intensity | 0.028 (***) | 0.031 (**) | 0.025 (***) | 0.016 (**) | ns | 0.019 (***) | ns |
| | | ns | | | 0.016 (**) | ns | 0.015 (**) | ns |
| Soil nutrients | Aluminum | ns | ns | ns | ns | ns | ns | ns |
| | Calcium | 0.016 (*) | ns | ns | 0.017 (**) | 0.016 (**) | 0.016 (*) | 0.023 (**) |
| | Iron | 0.018 (*) | ns | 0.161 (*) | 0.015 (*) | 0.013 (*) | 0.015 (*) | ns |
| | pH | ns | 0.019 (*) | 0.016(*) | 0.013 (*) | ns | ns | ns |
| | Potassium | ns | ns | ns | 0.015 (**) | ns | ns | 0.020 (**) |
| | Magnesium | 0.018 (*) | ns | ns | 0.016 (**) | ns | 0.016 (*) | ns |
| | Phosphorous | | 0.018 (*) | 0.017(*) | | | | |
| Topography | Elevation (m) | ns | ns | ns | ns | ns | ns | ns |
| | Topographic wetness index | ns | ns | ns | ns | ns | ns | ns |
| | Distance to stream (m) | 0.021 (**) | 0.019 (*) | 0.021 (*) | 0.014 (*) | ns | 0.013 (*) | ns |
| Dead biomass | Litter depth in 2022 | ns | ns | ns | ns | ns | ns | ns |
| | Duff depth in 2022 | ns | ns | ns | ns | ns | ns | ns |
| | Deadwood biomass | ns | ns | ns | ns | ns | ns | ns |
| Mortality | Distance-weighted basal area; 2014 – 2021 | ns | ns | ns | ns | 0.013 (*) | ns | ns |
| Live trees | Distance-weighted basal area in 2022 | 0.019 (*) | 0.022 (**) | 0.001 (*) | ns | ns | ns | ns |

copiotrophic bacteria (soil burn severity) and ectomycorrhizal fungi (delta normalized burn ratio [dNBR]). Distance to the nearest vernal stream was significant for all bacteria, as well as saprotrophic fungi. Distance-weighted overstory basal area was significant for bacteria only, whereas the amount of distance-weighted overstory mortality was important only for ectomycorrhizal fungi.

### 3.3. *Network topology, cohesion, and assembly processes*

Network topology and the identity of hub taxa were significantly different between burned and refugial samples (Fig. 7). As assessed by the adjusted Rand index (ARI), the composition node clusters were different ($P < 0.001$), for both the entire network (ARI = 0.232) and the largest connected component (ARI = 0.355). The graphlet correlation distance (GCD) was 0.479 between the entire network ($P = 0.001$), indicating substantial differences in entire network topology. There were 61 hub taxa shared between burned and refugial soils, 30 burned-only hub taxa, and 56 refugia-only hub taxa (Appendix C). There were 59 differential edges ($P < 0.05$) between nodes (47 hub taxa), by sample type (Fig. 7), with 22 that changed from positive (burned) to negative (refugia) associations, 28 that changed from negative (burned) to positive (refugia), and eight that had an increase in association strength (Appendix C). Notable hubs that had differential associations between burned and refugial soils included *Paenibacillus* (6 differential associations), *Kribbella* (4 differential associations), *Solirubrobacter* (3 differential assocations), *Cryptosporiopsis* (4 differenced associations), *Devriesia* (3 differenced associations), *Chalara* (2 differenced associations) (See Appendix B for full list). Burned communities had lower values of positive cohesion (0.15 vs. 0.21), |negative cohesion| (0.09 vs. 0.14), and total cohesion (0.25 vs. 0.35; Fig. 7b) than refugial communities ($P < 0.001$).

## 4. Discussion

Small-scale refugia maintain unique microbial communities that are richer and compositionally distinct from the stress-tolerant communities of burned soils, even nine years after fire (Fig. 5; Fig. 6). Our results consistently highlighted differing compositions between burned and refugia communities and did not support our hypothesis that refugia-to-burned dispersal of microbial communities would minimize the legacy of fire. Both direct and indirect fire effects changed community composition which suggests that variation in the scales and effects of wildfire (e.g., pyrodiversity) can influence the long-term composition of microbial functional guilds. Fireline intensity was associated with compositional differences in nearly all microbial communities, whereas the much more coarse-scale, remote-sensing dNBR burn severity metric failed to explain differences in microbial communities – except for ectomycorrhizal fungi, which likely responded to mortality of the overstory (Rodriguez-Ramos et al., 2021). Refugia may be desirable to promote or conserve on the landscape as life boats of unique microbial communities and more research is needed to identify to what extent refugia influence burned soil colonization in the immediate post-fire environment. Whereas prior work has identified near-immediate (e.g., days to weeks; Bruns et al., 2020) and short-term microbial changes between different burned and unburned forests (e.g., 3 y; Adkins et al., 2020), our study used co-occurring burned and refugia samples, thereby controlling for differences due to sampling from different forests. Importantly, our study is unique in that our co-occurring study design inherently captured the influence of bi-directional dispersion of communities between sample types and highlighted the ability of small-scale differences in fire behavior to have long-lasting impacts on co-occurring belowground microbial communities. The long-term ForestGEO dataset of the YFDP enabled us to assess the relative influence of aboveground forest neighborhoods on belowground communities and highlights the utility of leveraging long-term forest monitoring plots to investigate belowground microbial dynamics. Cumulatively, these results advance

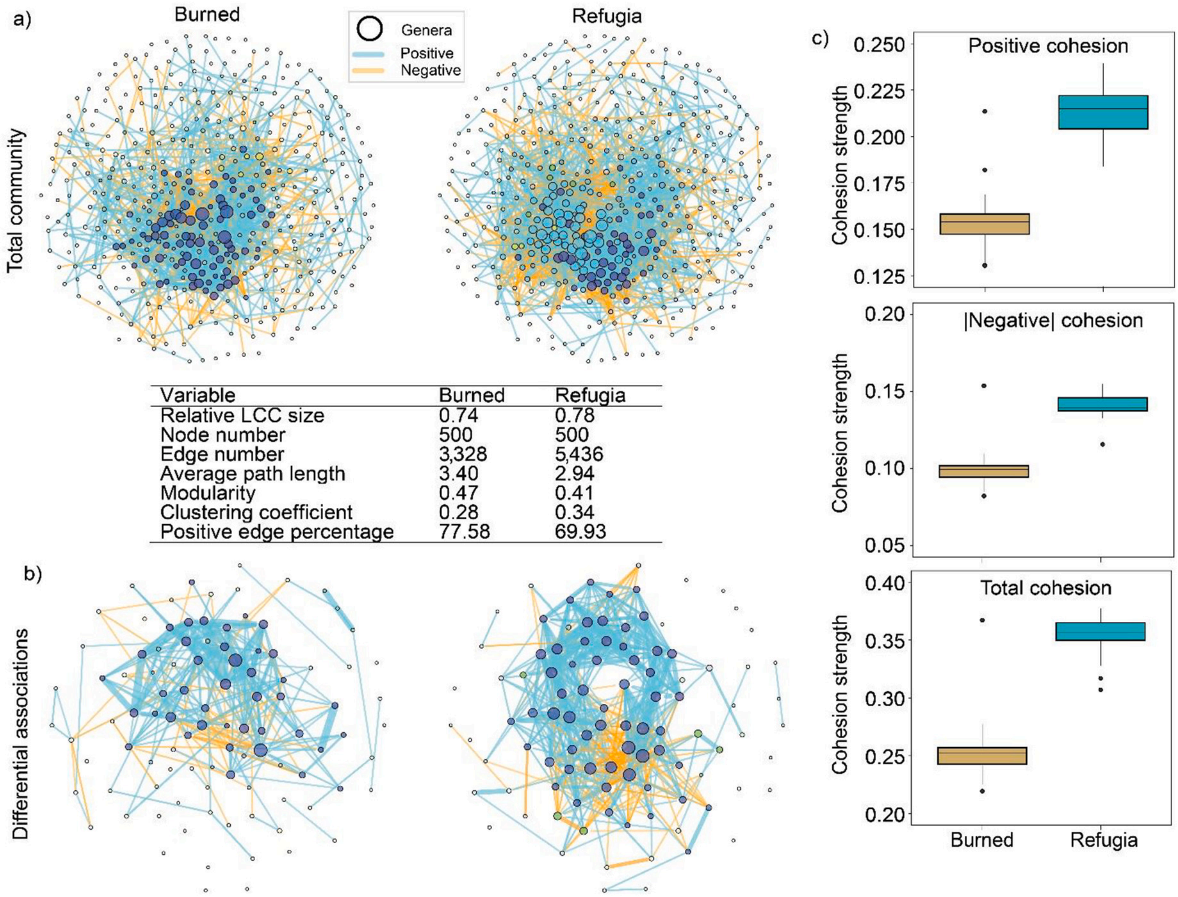

| Variable | Burned | Refugia |
|---|---|---|
| Relative LCC size | 0.74 | 0.78 |
| Node number | 500 | 500 |
| Edge number | 3,328 | 5,436 |
| Average path length | 3.40 | 2.94 |
| Modularity | 0.47 | 0.41 |
| Clustering coefficient | 0.28 | 0.34 |
| Positive edge percentage | 77.58 | 69.93 |

**Fig. 7.** Compositional networks and network cohesion for burned and refugia communities at the Yosemite Forest Dynamics Plot, CA, USA. (a) Circles (nodes) represent microbial genera, with size proportional to the degree of the node. Node color indicates cluster membership, with only clusters with ≥10 nodes represented. Only nodes present in burned and refugia soils are plotted. Orange (blue) lines represent negative (positive) correlations between nodes. (b) Differential associations ($P < 0.05$) between genera in burned and refugia taxa. (c) Positive, |negative|, and total cohesion for burned and refugia microbial communities.

an under-explored area in the effects of fire on belowground ecosystems.

Our results are representative of mixed-conifer ecosystems, which are adapted to frequent, mixed-severity fire regimes. Ecosystems with fire return intervals of decades to centuries (e.g., boreal or subalpine forests) may experience even greater differences between refugia and burned microbial communities owing to larger proportions of high burn severity and long successional times of decades to centuries (14–366 years, Cutler et al., 2017; but see Whitman et al., 2022). Climate change will likely result in more weather-driven fire and lower proportions of refugia within fire footprints (Mackey et al., 2021) even as wildfires burn into ecosystems that previously burned only infrequently (Alizadeh et al., 2021). Thus, we might expect a lower proportion of fire refugia under warmer, drier climates as weather-driven fire behavior and effects become more homogenous (Wasserman and Mueller, 2023). Increasing homogeneity of fire effects may in turn alter the distribution of woody species whose range is jointly influenced by climate and existing fire regimes (Birch and Lutz, 2023; van Wagtendonk et al., 2020). More long-term, spatially-explicit research (e.g., Lutz et al., 2018) is needed to identify the role of small-scale refugia as life-boats for fire-sensitive and late-successional species, both above- and below-ground.

### *4.1. Soil microbial communities were influenced by direct and indirect fire effects*

Were the differences in burned and refugia communities driven primarily by direct or indirect impacts of wildfire? Pre-fire surface fuel loadings were an average of 192 Mg ha$^{-1}$ (Cansler et al., 2019), and smoldering duff combustion likely induced substantial soil heating (>60C) in the upper 5 cm of the mineral soil for several hours, with longer durations (e.g., 10–22 h) under drier soil moistures (Busse et al., 2023; Hartford and Frandsen, 1992). In addition to killing fine roots and injuring microbes (Busse et al., 2023) these temperatures may also have altered the physical and chemical structure of the soil. Whereas many macronutrients can begin to be volatilized in high intensity fires that produce soil heating >200 °C (Agbeshie et al., 2022), the 2013 Rim Fire burned at relatively moderate intensities in the YFDP; therefore, we expect that only soils adjacent to smoldering large deadwood (≥ 7.6 cm diameter) experienced sufficient heating to volatize nutrients (Monsanto and Agee, 2008).

Delayed fire effects have likely continued to influence the development and dispersal of microbial communities. The Rim fire caused distinct shifts in the dynamics and mortality factors of the overstory which have persisted in the decade after fire (Furniss et al., 2020). The elevated tree mortality rates in the decade after fire have likely favored saprotrophic microbes, relative to symbiotic or pathogenic guilds (Pérez-Izquierdo et al., 2021). As well, post-fire changes to soil albedo (Bodí et al., 2014; Weltzin et al., 2005) caused by the consumption of the forest floor, may have induced long-term soil warming and loss of soil organic carbon (Harden et al., 2006; Zosso et al., 2023) and generally increased stress in burned soils until the accumulation of a new forest floor (Iverson and Hutchinson, 2002). This is supported by the starkly elevated saprotrophic richness in refugia whose forest floor has been continually accumulating and decomposing since at least 1899 (Fig. 6; Table A.5). However, we expected that these disturbances and stresses would have been mitigated with time through the gradual deposition of a new forest floor layer via litterfall and decomposition, and commensurate increases in carbon and nutrient inputs to the mineral soil.

### 4.2. More cohesive refugia communities: Potential causes and consequences

Refugial communities had 6 % more negative interactions and greater cohesion than burned communities, which suggests that refugial communities may be more stable and have greater resistance to future, non-fire disturbance (Fig. 7). Greater proportions of negative associations, indicative of niche differentiation or competition, have been implicated in promoting richer, more resistant communities (Coyte et al., 2015) which may in part explain the higher diversity in refugia (Fig. 6). The greater proportion of facilitation (positive) interactions in burned communities supports the stress-gradient hypothesis that facilitative interactions will dominate in more stressful and species-poor communities (e.g., burned soils). Changes to the type and abundance of nutrients, soil temperature, and loss of roots after fire may be expected to broadly increase the stress in burned soils and thus increase the relative importance of facilitative interactions in the belowground community.

Notable differences in network topology may also be a consequence, or cause, of the greater richness and altered composition between burned and refugia soils. We might expect that belowground successional processes result in turnover or accumulation of species and spores with time (Birch et al., 2021; Sauvadet et al., 2019) which contribute to differences in network topology from community turnover and new taxa additions. Whereas many hub taxa were shared between soil types, both soil types had unique hubs with differential associations (Fig. 7; Appendix B). These may be due to differences in the abiotic environment such as nutrient availability, altered associations with plants in disturbed communities (de Vries et al., 2018), or the loss or gain of keystone microbes (Herren and McMahon, 2018).

### 4.3. Utility of refugia for preserving and promoting biodiversity

Small-scale refugia may act as an important lifeboat for pyro-phobic and late successional microbes, persevering species and communities that may subsequently re-colonize burned soils (Franklin et al., 2000). In addition to harboring potentially beneficial symbiotic or saprotrophic microbes, refugia also harbored elevated pathogenic microbial diversity, possibly owing to greater abundances of hosts (Parker et al., 2006) or avoidance of direct fire effects that would otherwise kill fire-sensitive pathogens (Reaves et al., 1990). Surprisingly, despite a high compositional overlap, the persistent differences in refugia communities relative to burned areas indicate that homogenizing dispersal processes or succession were not yet strong enough to overcome potential priority effects or fire-induced changes in habitats (Dini-Andreote et al., 2015). Microbial dispersal after fire can alter long-term community trajectories through priority effects and by altering community assembly (Barbour et al., 2023). Likely, taxa dispersed from refugia into neighboring burned communities but burned communities maintained unique compositions owing to their altered abiotic environment (Adkins et al., 2020). Future research on the short- and long-term dynamics of refugial communities may reveal how bi-directional dispersion influences microbial community assembly.

An implicit assumption of this work is that refugia are representative of the pre-fire microbial community, though the refugial communities may represent a departure from historic communities shaped by frequent fire. Before the implementation of modern fire suppression policy, more refugia may have remained after fires in mixed-conifer forests because of the historically (pre-Euro-American settlement) more frequent natural and cultural fires. Prior fire regimes were conducive to milder fire effects including patchier fire spread, greater large-diameter tree survival (Lutz et al., 2009), and lower deadwood loadings with commensurately lower soil heating during fires (Markwith and Paudel, 2022).

### 4.4. Management recommendations for refugia

In systems at risk of uncharacteristic, homogenous fire effects (e.g., wind-driven or crown fire in fire-suppressed mixed-conifer ecosystems), management interventions may reduce surface fuels and promote greater pyrodiversity and help create refugia. Treatments, such as mastication or thinning, that cause greater spatial variability in large deadwood or forest floor fuels may be particularly desirable as these fuels are typically autocorrelated over scales of meters to many dozens of meters (Keane, 2016; Vakili et al., 2016), and contribute to substantial energy release, thereby influencing fire behavior (Birch et al., 2023a).

Wildfires or prescribed fires that burn during moderate to marginal weather conditions are likely to promote refugia (Donovan et al., 2024; Price et al., 2003) and induce fuel-driven fire behavior and soil heating commensurate with spatial variation in fuel loadings. Naturally ignited wildfires managed, at least in part, for resource benefit (Fillmore et al., 2024) would often burn under relatively moderate conditions (North et al., 2021) which could be expected to result in a larger proportion of refugia than would occur where suppression were prioritized. These activities, along with broader ecosystem conservation, may be important for preserving reservoirs of microbial diversity and fire-sensitive ecosystems (Larson et al., 2022).

### 4.5. Conclusion

Wildfire behavior produces enduring and variable influences on belowground community composition and richness that may go undetected by coarse-scale approaches of assessing wildfire effects. Given the role of variable fire behavior and effects in directly and indirectly influencing microbial communities, variability may enhance belowground diversity on the landscape and promote a greater variety of both pyrophobic and pyrophilic communities. As wildfires become increasingly large and more homogenously high-severity, unburned refugia may become even more important for maintaining the full diversity of microbial communities on the landscape.

## CRediT authorship contribution statement

**Joseph D. Birch:** Writing – review & editing, Writing – original draft, Visualization, Methodology, Funding acquisition, Formal analysis, Data curation, Conceptualization. **James A. Lutz:** Writing – review & editing, Writing – original draft, Resources, Data curation, Conceptualization. **Matthew B. Dickinson:** Writing – review & editing, Writing – original draft, Resources. **James Franklin:** Writing – review & editing, Methodology. **Andrew J. Larson:** Writing – review & editing. **Mark E. Swanson:** Writing – review & editing. **Jessica R. Miesel:** Writing – review & editing, Resources, Project administration, Funding acquisition, Conceptualization.

## Funding

This project was supported by the California Department of Forestry and Fire Protection (Grant number 8GG19804) as part of the California Climate Investments Program, McIntire-Stennis (Project MICL06033), and a Michigan State University Ecology, Evolution, and Behavior seed grant to JRM and JDB. The Yosemite Forest Dynamics Plot was funded by Utah State University, the University of Montana, Washington State University, and the Utah Agricultural Experiment station which has designated this as paper #9752.

## Declaration of competing interest

The authors declare the following financial interests/personal relationships which may be considered as potential competing interests:

Jessica Miesel reports financial support was provided by California Department of Forestry and Fire Protection. Jessica Miesel reports financial support was provided by Michigan State University Ecology, Evolution, and Behavior. James Lutz reports financial support was provided by Utah Agricultural Experiment station. If there are other authors, they declare that they have no known competing financial interests or personal relationships that could have appeared to influence the work reported in this paper.

## *Acknowledgments*

We appreciate the work of H. Haley in analyzing 2013 Rim fire behavior videos. We thank Dr. Jeff Loveland for his assistance with land-use history. Research was conducted under annual permits from the National Park Service for study #YOSE-00051. We acknowledge and very much appreciate the contribution of Yosemite National Park managers in supporting our work.

## Appendix A. Supplementary data

Supplementary data to this article can be found online at https://doi.org/10.1016/j.scitotenv.2025.178677.

## Data availability

All fire behavior data is available at frames.gov/fbat. Analytical code available upon request.

## References

Abarenkov, K., Zirk, A., Piirmann, T., Pöhönen, R., Ivanov, F., Nilsson, R.H., et al., 2023. UNITE general FASTA release for Fungi 2. UNITE Community. https://doi.org/10.15156/BIO/2938068.

Adkins, J., Docherty, K.M., Gutknecht, J.L.M., Miesel, J.R., 2020. How do soil microbial communities respond to fire in the intermediate term? Investigating direct and indirect effects associated with fire occurrence and burn severity. Sci. Total Environ. 745, 140957. https://doi.org/10.1016/j.scitotenv.2020.140957.

Adkins, J., Docherty, K.M., Miesel, J.R., 2022. Copiotrophic bacterial traits increase with burn severity one year after a wildfire. Frontiers in forests and global. Change 5. https://doi.org/10.3389/ffgc.2022.873527.

Agbeshie, A.A., Abugre, S., Atta-Darkwa, T., Awuah, R., 2022. A review of the effects of forest fire on soil properties. J. For. Res. 33, 1419–1441. https://doi.org/10.1007/s11676-022-01475-4.

Alexander, M.E., Cruz, M.G., 2012. Interdependencies between flame length and fireline intensity in predicting crown fire initiation and crown scorch height. Int. J. Wildland Fire 21, 95–113. https://doi.org/10.1071/WF11001.

Alizadeh, M.R., Abatzoglou, J.T., Luce, C.H., Adamowski, J.F., Farid, A., Sadegh, M., 2021. Warming enabled upslope advance in western US forest fires. Proc. Natl. Acad. Sci. 118, e2009717118. https://doi.org/10.1073/pnas.2009717118.

Baldeck, C.A., Harms, K.E., Yavitt, J.B., John, R., Turner, B.L., Valencia, R., et al., 2013. Soil resources and topography shape local tree community structure in tropical forests. Proc. R. Soc. B Biol. Sci. 280, 20122532. https://doi.org/10.1098/rspb.2012.2532.

Barbour KM, Weihe C, Walters KE, Martiny JBH. Testing the contribution of dispersal to microbial succession following a wildfire. mSystems 2023; 8: e00579–23. doi:https://doi.org/10.1128/msystems.00579-23.

Barth, M.A.F., Larson, A.J., Lutz, J.A., 2015. A forest reconstruction model to assess changes to Sierra Nevada mixed-conifer forest during the fire suppression era. For. Ecol. Manag. 354, 104–118. https://doi.org/10.1016/j.foreco.2015.06.030.

Bartoń, K., 2022. Multi-model inference, Version 1.46.0. https://cran.r-project.org/web//packages//MuMIn/index.html.

Beals, K.K., Scearce, A.E., Swystun, A.T., Schweitzer, J.A., 2022. Belowground mechanisms for oak regeneration: interactions among fire, soil microbes, and plant community alter oak seedling growth. For. Ecol. Manag. 503, 119774. https://doi.org/10.1016/j.foreco.2021.119774.

Berndt HW, Gibbons RD. Root distribution of some native trees and understory plants growing on three sites within ponderosa pine watersheds in Colorado. In: Agriculture USDo, editor. 37. Rocky Mountain Forest and Range Experiment Station, Fort Collins, CO, 1958.

Birch, J.D., Dickinson, M.B., Reiner, A., Knapp, E.E., Dailey, S.N., Ewell, C., et al., 2023a. Heading and backing fire behaviours mediate the influence of fuels on wildfire energy. Int. J. Wildland Fire 32, 1244–1261. https://doi.org/10.1071/WF22010.

Birch, J.D., Lutz, J.A., 2023. Fire regimes of Utah: the past as prologue. Fire 6, 423.

Birch, J.D., Lutz, J.A., Karst, J., 2022. Dancing with Douglas-fir: determinism dominates fungal community assembly processes. J. Ecol. 110, 1857–1870. https://doi.org/10.1111/1365-2745.13910.

Birch, J.D., Lutz, J.A., Struckman, S., Miesel, J.R., Karst, J., 2023b. Large-diameter trees and deadwood correspond with belowground ectomycorrhizal fungal richness. Ecol. Process. 12, 3. https://doi.org/10.1186/s13717-022-00415-8.

Birch, J.D., Lutz, J.A., Turner, B.L., Karst, J., 2021. Divergent, age-associated fungal communities of *Pinus flexilis* and *Pinus longaeva*. For. Ecol. Manag. 494, 119277. https://doi.org/10.1016/j.foreco.2021.119277.

Blomdahl, E.M., Kolden, C.A., Meddens, A.J.H., Lutz, J.A., 2019. The importance of small fire refugia in the Central Sierra Nevada, California, USA. For. Ecol. Manag. 432, 1041–1052. https://doi.org/10.1016/j.foreco.2018.10.038.

Bodí, M.B., Martin, D.A., Balfour, V.N., Santín, C., Doerr, S.H., Pereira, P., et al., 2014. Wildland fire ash: production, composition and eco-hydro-geomorphic effects. Earth Sci. Rev. 130, 103–127. https://doi.org/10.1016/j.earscirev.2013.12.007.

Bradshaw, L., McCormick, E., 2000. FireFamily Plus user's Guide, Version 2.0. Gen. Tech. Rep. RMRS-GTR-67.. US Department of Agriculture, Forest Service, Rocky Mountain Research Station, Ogden, UT, p. 67.

Brady, M.K., Dickinson, M.B., Miesel, J.R., Wonkka, C.L., Kavanagh, K.L., Lodge, A.G., et al., 2022. Soil heating in fire (SheFire): a model and measurement method for estimating soil heating and effects during wildland fires. Ecol. Appl. 32, e2627. https://doi.org/10.1002/eap.2627.

Bruns, T.D., Chung, J.A., Carver, A.A., Glassman, S.I., 2020. A simple pyrocosm for studying soil microbial response to fire reveals a rapid, massive response by *Pyronema* species. PLoS One 15, e0222691. https://doi.org/10.1371/journal.pone.0222691.

Busse, M., Shestak, C.J., Hubbert, K.R., 2023. Soil nutrient release and microbial changes after burning of masticated fuels. Soil Sci. Soc. Am. J. 87, 172–181. https://doi.org/10.1002/saj2.20489.

Byram, G.M., 1959. Combustion of forest fuels. In: Davis, K. (Ed.), Forest Fire: Control and Use. New York, McGraw-Hill, pp. 61–89.

Callahan, B.J., McMurdie, P.J., Rosen, M.J., Han, A.W., Johnson, A.J.A., Holmes, S.P., 2016. DADA2: high-resolution sample inference from Illumina amplicon data. Nat. Methods 13, 581–583. https://doi.org/10.1038/nmeth.3869.

Cansler, C.A., Swanson, M.E., Furniss, T.J., Larson, A.J., Lutz, J.A., 2019. Fuel dynamics after reintroduced fire in an old-growth Sierra Nevada mixed-conifer forest. Fire Ecol. 15, 16. https://doi.org/10.1186/s42408-019-0035-y.

Cousins, S.J.M., Battles, J.J., Sanders, J.E., York, R.A., 2015. Decay patterns and carbon density of standing dead trees in California mixed conifer forests. For. Ecol. Manag. 353, 136–147. https://doi.org/10.1016/j.foreco.2015.05.030.

Coyte, K.Z., Schluter, J., Foster, K.R., 2015. The ecology of the microbiome: networks, competition, and stability. Science 350, 663–666. https://doi.org/10.1126/science.aad2602.

Csárdi, G., Nepusz, T., 2006. The igraph software package for complex network research. InterJournal Complex Syst 1695.

Csárdi G, Nepusz T, Traag V, Horvát S, Zanini F, Noom D, et al. igraph: Network analysis and visualization in R. 2024. Version 2.0. 2 https://cran.r-project.org/web//packages//igraph/index.html.

Cutler, N.A., Arróniz-Crespo, M., Street, L.E., Jones, D.L., Chaput, D.L., DeLuca, T.H., 2017. Long-term recovery of microbial communities in the boreal bryosphere following fire disturbance. Microb. Ecol. 73, 75–90. https://doi.org/10.1007/s00248-016-0832-7.

Davies, S.J., Abiem, I., Abu Salim, K., Aguilar, S., Allen, D., Alonso, A., et al., 2021. ForestGEO: understanding forest diversity and dynamics through a global observatory network. Biol. Conserv. 253, 108907. https://doi.org/10.1016/j.biocon.2020.108907.

Day, N.J., Cumming, S.G., Dunfield, K.E., Johnstone, J.F., Mack, M.C., Reid, K.A., et al., 2020. Identifying functional impacts of heat-resistant fungi on boreal forest recovery after wildfire. Frontiers in forests and global. Change 3. https://doi.org/10.3389/ffgc.2020.00068.

de Vries, W., Reinds, G.J., Bierkens, M.F.P., 2009. Assessment of the optimal time interval for repeated soil surveys at intensively monitored forest plots. J. Environ. Monitor. 11, 2009–2021. https://doi.org/10.1039/B909480F.

de Vries, F.T., Griffiths, R.I., Bailey, M., Craig, H., Girlanda, M., Gweon, H.S., et al., 2018. Soil bacterial networks are less stable under drought than fungal networks. Nat. Commun. 9, 3033. https://doi.org/10.1038/s41467-018-05516-7.

Dickinson, M.B., Johnson, E.A., 2004. Temperature-dependent rate models of vascular cambium cell mortality. Can. J. For. Res. 34, 546–559. https://doi.org/10.1139/x03-223.

Dickinson, M.B., Johnson, E.A., Artiaga, R., 2013. Fire spread probabilities for experimental beds composed of mixedwood boreal forest fuels. Can. J. For. Res. 43, 321–330. https://doi.org/10.1139/cjfr-2012-0291.

Dini-Andreote, F., Stegen, J.C., van Elsas, J.D., Salles, J.F., 2015. Disentangling mechanisms that mediate the balance between stochastic and deterministic processes in microbial succession. Proc. Natl. Acad. Sci. 112, E1326–E1332. https://doi.org/10.1073/pnas.1414261112.

Donovan, V.M., Scholtz, R., Wonkka, C.L., 2024. Fire refugia patch dynamics differ between prescribed fires and wildfires in longleaf pine savanna. For. Ecol. Manag. 569, 122179. https://doi.org/10.1016/j.foreco.2024.122179.

Fillmore, S.D., McCaffrey, S., Bean, R., Evans, A.M., Iniguez, J., Thode, A., Smith, A.M., Thompson, M.P., 2024. Factors influencing wildfire management decisions after the 2009 US federal policy update. Inter. J. Wildland Fire 33 (1).

Fox, J., Weisberg, S., 2018. An R Companion to Applied Regression. Sage Publications.

Fox, S., Sikes, B.A., Brown, S.P., Cripps, C.L., Glassman, S.I., Hughes, K., et al., 2022. Fire as a driver of fungal diversity — a synthesis of current knowledge. Mycologia 114, 215–241. https://doi.org/10.1080/00275514.2021.2024422.

Franklin, J.F., Lindenmayer, D., MacMahon, J.A., McKee, A., Magnuson, J., Perry, D.A., et al., 2000. Threads of continuity. Conserv. Biol. Pract. 1, 8–16.

Fukuyama J. phyloseqGraphTest: graph-based permutation tests for microbiome data. 2023. Version 0.1.1. https://CRAN.R-project.org/package=phyloseqGraphTest.

Furniss, T.J., Larson, A.J., Kane, V.R., Lutz, J.A., 2020. Wildfire and drought moderate the spatial elements of tree mortality. Ecosphere 11, e03214. https://doi.org/10.1002/ecs2.3214.

Gao, C., Xu, L., Montoya, L., Madera, M., Hollingsworth, J., Chen, L., et al., 2022. Co-occurrence networks reveal more complexity than community composition in resistance and resilience of microbial communities. Nat. Commun. 13, 3867. https://doi.org/10.1038/s41467-022-31343-y.

Gill, A.M., 1974. Toward an understanding of fire-scar formation: field observation and laboratory simulation. For. Sci. 20, 198–205. https://doi.org/10.1093/forestscience/20.3.198.

Glassman SI, Martiny JBH. Broadscale ecological patterns are robust to use of exact sequence variants versus operational taxonomic units. mSphere 2018; 3: https://doi.org/10.1128/msphere.00148-18. doi:https://doi.org/10.1128/msphere.00148-18.

Gräler, B., Pebesma, E.J., Heuvelink, G.B., 2016. Spatio-temporal interpolation using gstat. The R Journal 8, 204.

Harden, J., Manies, K., Turetsky, M.R., JC N., 2006. Effects of wildfire and permafrost on soil organic matter and soil climate in interior Alaska. Glob. Chang. Biol. 12, 2391–2403. https://doi.org/10.1111/j.1365-2486.2006.01255.x.

Harmon ME, Woodall CW, Fasth B, Sexton J. Woody Detritus Density and Density Reduction Factors for Tree Species in the United States: A Synthesis. USDA For. Serv. Gen. Tech. Rep. NRS-29 2008.

Hartford, R., Frandsen, W., 1992. When it's hot, it's hot... Or maybe It's not! (surface flaming may not portend extensive soil heating). Int. J. Wildland Fire 2, 139–144. https://doi.org/10.1071/WF9920139.

Hernandez, D.J., David, A.S., Menges, E.S., Searcy, C.A., Afkhami, M.E., 2021. Environmental stress destabilizes microbial networks. ISME J. 15, 1722–1734. https://doi.org/10.1038/s41396-020-00882-x.

Herren, C.M., McMahon, K.D., 2018. Keystone taxa predict compositional change in microbial communities. Environ. Microbiol. 20, 2207–2217. https://doi.org/10.1111/1462-2920.14257.

Hočevar, T., Demšar, J., 2016. Computation of graphlet orbits for nodes and edges in sparse graphs. J. Stat. Softw. 71, 1–24. https://doi.org/10.18637/jss.v071.i10.

Hubert, L., Arabie, P., 1985. Comparing partitions. Journal of classification 2, 193–218.

Hunter, M.E., Robles, M.D., 2020. Tamm review: the effects of prescribed fire on wildfire regimes and impacts: a framework for comparison. For. Ecol. Manag. 475, 118435. https://doi.org/10.1016/j.foreco.2020.118435.

Ihrmark, K., Bödeker, I.T.M., Cruz-Martinez, K., Friberg, H., Kubartova, A., Schenck, J., et al., 2012. New primers to amplify the fungal ITS2 region – evaluation by 454-sequencing of artificial and natural communities. FEMS Microbiol. Ecol. 82, 666–677. https://doi.org/10.1111/j.1574-6941.2012.01437.x.

Iverson, L., Hutchinson, T., 2002. Soil temperature and moisture fluctuations during and after prescribed fire in mixed-oak forests, USA. Nat. Areas J. 22, 296–304. https://doi.org/10.1038/s41561-023-01142-1.

Johnson, E.A., 1996. Fire and Vegetation Dynamics: Studies from the North American Boreal Forest. Cambridge University Press, Cambridge, UK.

Jones, G.M., Tingley, M.W., 2022. Pyrodiversity and biodiversity: a history, synthesis, and outlook. Divers. Distrib. 28, 386–403. https://doi.org/10.1111/ddi.13280.

Kane, V.R., Cansler, C.A., Povak, N.A., Kane, J.T., McGaughey, R.J., Lutz, J.A., et al., 2015. Mixed severity fire effects within the rim fire: relative importance of local climate, fire weather, topography, and forest structure. For. Ecol. Manag. 358, 62–79. https://doi.org/10.1016/j.foreco.2015.09.001.

Kassambara A. ggpubr: 'ggplot2' based publication ready plots. 2023. Version 0.6.0. https://cran.r-project.org/package=ggpubr.

Keane, R.E., 2016. Spatiotemporal variability of wildland fuels in US northern Rocky Mountain forests. Forests 7, 129.

Keeley, J.E., 2009. Fire intensity, fire severity and burn severity: a brief review and suggested usage. Int. J. Wildland Fire 18, 116–126. https://doi.org/10.1071/WF07049.

Key CH, Benson NC. Landscape assessment (LA). FIREMON: Fire effects monitoring and inventory system 2006; 164: LA-1-55.

Kipfer, T., Moser, B., Egli, S., Wohlgemuth, T., Ghazoul, J., 2011. Ectomycorrhiza succession patterns in *Pinus sylvestris* forests after stand-replacing fire in the Central Alps. Oecologia 167, 219–228. https://doi.org/10.1007/s00442-011-1981-5.

Kolden, C.A., Lutz, J.A., Key, C.H., Kane, J.T., van Wagtendonk, J.W., 2012. Mapped versus actual burned area within wildfire perimeters: characterizing the unburned. For. Ecol. Manag. 286, 38–47. https://doi.org/10.1016/j.foreco.2012.08.020.

Kutiel, P., Naveh, Z., 1987. The effect of fire on nutrients in a pine forest soil. Plant Soil 104, 269–274. https://doi.org/10.1007/BF02372541.

Larson, A.J., Jeronimo, S.M.A., Hessburg, P.F., Lutz, J.A., Povak, N.A., Cansler, C.A., et al., 2022. Tamm review: ecological principles to guide post-fire forest landscape management in the inland Pacific and northern Rocky Mountain regions. For. Ecol. Manag. 504, 119680. https://doi.org/10.1016/j.foreco.2021.119680.

Liu, S., Yu, H., Yu, Y., Huang, J., Zhou, Z., Zeng, J., et al., 2022. Ecological stability of microbial communities in Lake Donghu regulated by keystone taxa. Ecol. Indic. 136, 108695. https://doi.org/10.1016/j.ecolind.2022.108695.

Lutz, J.A., Larson, A.J., Swanson, M.E., 2018. Advancing fire science with large forest plots and a long-term multidisciplinary approach. Fire 1, 5. https://doi.org/10.3390/fire1010005.

Lutz, J.A., Larson, A.J., Swanson, M.E., Freund, J.A., 2012. Ecological importance of large-diameter trees in a temperate mixed-conifer forest. PLoS One 7, e36131. https://doi.org/10.1371/journal.pone.0036131.

Lutz, J.A., Struckman, S., Furniss, T.J., Cansler, C.A., Germain, S.J., Yocom, L.L., et al., 2020. Large-diameter trees dominate snag and surface biomass following reintroduced fire. Ecol. Process. 9, 41. https://doi.org/10.1186/s13717-020-00243-8.

Lutz, J.A., van Wagtendonk, J.W., Franklin, J.F., 2009. Twentieth-century decline of large-diameter trees in Yosemite National Park, California, USA. For. Ecol. Manag. 257, 2296–2307. https://doi.org/10.1016/j.foreco.2009.03.009.

Mackey, B., Lindenmayer, D., Norman, P., Taylor, C., Gould, S., 2021. Are fire refugia less predictable due to climate change? Environ. Res. Lett. 16, 114028. https://doi.org/10.1088/1748-9326/ac2e88.

Markwith, S.H., Paudel, A., 2022. Beyond pre-Columbian burning: the impact of firewood collection on forest fuel loads. Can. J. For. Res. 52, 365–371. https://doi.org/10.1139/cjfr-2021-0207.

Martin, M., 2011. Cutadapt removes adapter sequences from high-throughput sequencing reads. 2011 (17), 3. https://doi.org/10.14806/ej.17.1.200.

McLaren, M.R., Callahan, B.J., 2021. Silva 138.1 prokaryotic SSU taxonomic training data formatted for DADA2. Zenodo. https://doi.org/10.5281/zenodo.4587955.

McMurdie, P.J., Holmes, S., 2013. Phyloseq: an R package for reproducible interactive analysis and graphics of microbiome census data. PLoS One 8, e61217. https://doi.org/10.1371/journal.pone.0061217.

Meddens, A.J.H., Kolden, C.A., Lutz, J.A., Smith, A.M.S., Cansler, C.A., Abatzoglou, J.T., et al., 2018. Fire refugia: what are they, and why do they matter for global change? BioScience 68, 944–954. https://doi.org/10.1093/biosci/biy103.

Miesel, J.R., Hockaday, W.C., Kolka, R.K., Townsend, P.A., 2015. Soil organic matter composition and quality across fire severity gradients in coniferous and deciduous forests of the southern boreal region. J. Geophys. Res. Biogeosci. 120, 1124–1141. https://doi.org/10.1002/2015JG002959.

Miller, J.D., Thode, A.E., 2007. Quantifying burn severity in a heterogeneous landscape with a relative version of the delta normalized burn ratio (dNBR). Remote Sens. Environ. 109, 66–80. https://doi.org/10.1016/j.rse.2006.12.006.

Monsanto, P.G., Agee, J.K., 2008. Long-term post-wildfire dynamics of coarse woody debris after salvage logging and implications for soil heating in dry forests of the eastern cascades. Washington. Forest Ecology and Management 255, 3952–3961. https://doi.org/10.1016/j.foreco.2008.03.048.

National Weather Service, 2023. Hourly climate data: station ID FA60C528. U.S. Department of the Interior GS, and U.S. department of. Agriculture.

National Wildfire Coordinating Group. Fire Behavior Analyst. Position description: FIre Behavior Analyst. 2024. National Wildfire Coordinating Group, 2024.

North, M.P., York, R.A., Collins, B.M., Hurteau, M.D., Jones, G.M., Knapp, E.E., et al., 2021. Pyrosilviculture needed for landscape resilience of dry Western United States forests. J. For. 119, 520–544. https://doi.org/10.1093/jofore/fvab026.

Oksanen J, Simpson G, Blanchet F, Kindt R, Legendre P, Minchin P, et al. vegan: community ecology package. 2023. Version 2.6–4. https://cran.r-project.org/web//packages//vegan/index.html.

Parker, T.J., Clancy, K.M., Mathiasen, R.L., 2006. Interactions among fire, insects and pathogens in coniferous forests of the interior western United States and Canada. Agric. For. Entomol. 8, 167–189. https://doi.org/10.1111/j.1461-9563.2006.00305.x.

Parsons A, Robichaud PR, Lewis SA, Napper C, Clark JT. Field guide for mapping post-fire soil burn severity. 243. U.S. Department of Agriculture, Forest Service, Rocky Mountain Research Station, 2010. doi:https://doi.org/10.2737/rmrs-gtr-243.

Pebesma, E.J., 2004. Multivariable geostatistics in S: the gstat package. Comput. Geosci. 30, 683–691. https://doi.org/10.1016/j.cageo.2004.03.012.

Pérez-Izquierdo, L., Clemmensen, K.E., Strengbom, J., Granath, G., Wardle, D.A., Nilsson, M.-C., et al., 2021. Crown-fire severity is more important than ground-fire severity in determining soil fungal community development in the boreal forest. J. Ecol. 109, 504–518. https://doi.org/10.1111/1365-2745.13529.

Pérez-Valera, E., Goberna, M., Verdú, M., 2019. Fire modulates ecosystem functioning through the phylogenetic structure of soil bacterial communities. Soil Biol. Biochem. 129, 80–89. https://doi.org/10.1016/j.soilbio.2018.11.007.

Peschel, S., 2023. NetCoMi: Network Construction and Comparison for Microbiome Data, Version 1.1.0. https://github.com/stefpeschel/NetCoMi.

Peschel, S., Müller, C.L., von Mutius, E., Boulesteix, A.-L., Depner, M., 2020. NetCoMi: network construction and comparison for microbiome data in R. Brief. Bioinform. 22. https://doi.org/10.1093/bib/bbaa290.

Põlme, S., Abarenkov, K., Henrik Nilsson, R., Lindahl, B.D., Clemmensen, K.E., Kauserud, H., et al., 2020. FungalTraits: a user-friendly traits database of fungi and fungus-like stramenopiles. Fungal Divers. 105, 1–16. https://doi.org/10.1007/s13225-020-00466-2.

Price, O., Russell-Smith, J., Edwards, A., 2003. Fine-scale patchiness of different fire intensities in sandstone heath vegetation in northern Australia. Int. J. Wildland Fire 12, 227–236. https://doi.org/10.1071/WF03040.

Pulido-Chavez, M.F., Alvarado, E.C., DeLuca, T.H., Edmonds, R.L., Glassman, S.I., 2021. High-severity wildfire reduces richness and alters composition of ectomycorrhizal fungi in low-severity adapted ponderosa pine forests. For. Ecol. Manag. 485, 118923. https://doi.org/10.1016/j.foreco.2021.118923.

Qannari, E.M., Courcoux, P., Faye, P., 2014. Significance test of the adjusted Rand index. Application to the free sorting task. Food Qual. Prefer. 32, 93–97. https://doi.org/10.1016/j.foodqual.2013.05.005.

R Core Team. R: A language and environment for statistical computing. 2022. Version 4.2.1. https://www.r-project.org/.

R Studio Team. Studio: Integrated Development for R. 2023. Version 2023.06.02. https://posit.co/downloads/.

Reaves, J., Shaw III, C., Mayfield, J., 1990. The effects of *Trichoderma* spp. isolated from burned and non-burned forest soils on the growth and development of *Armillaria ostoyae* in culture. Northwest Science 64, 39–44.

Reiner, A.L., Ewell, C.M., Fites-Kaufman, J.A., Dailey, S.N., Noonan-Wright, E.K., Norman, T.P., et al., 2021. Fire behavior assessment Team: in-fire videos. United States department of. Agriculture. https://doi.org/10.2737/RDS-2021-0069.

Response, Burned Area Emergency, 2013. Soil Burn Severity. Rim fire, United States Department of Agriculture. https://burnseverity.cr.usgs.gov/baer/baer-imagery-support-data-download.

Rodriguez-Ramos, J.C., Cale, J.A., Cahill Jr., J.F., Simard, S.W., Karst, J., Erbilgin, N., 2021. Changes in soil fungal community composition depend on functional group and forest disturbance type. New Phytol. 229, 1105–1117. https://doi.org/10.1111/nph.16749.

Rosenberg, B., Kemeny, G., Switzer, R.C., Hamilton, T.C., 1971. Quantitative evidence for protein denaturation as the cause of thermal death. Nature 232, 471–473. https://doi.org/10.1038/232471a0.

Safford, H.D., Stevens, J.T., 2017. Natural Range of Variation for Yellow Pine and Mixed-Conifer Forests in the Sierra Nevada, Southern Cascades, and Modoc and Inyo National Forests. California, USA.

Sauvadet, M., Fanin, N., Chauvat, M., Bertrand, I., 2019. Can the comparison of above- and below-ground litter decomposition improve our understanding of bacterial and fungal successions? Soil Biol. Biochem. 132, 24–27. https://doi.org/10.1016/j.soilbio.2019.01.022.

Steindorff, A.S., Carver, A., Calhoun, S., Stillman, K., Liu, H., Lipzen, A., et al., 2021. Comparative genomics of pyrophilous fungi reveals a link between fire events and developmental genes. Environ. Microbiol. 23, 99–109. https://doi.org/10.1111/1462-2920.15273.

Tamjidi, J., Lutz, J.A., 2020. Soil enzyme activity and soil nutrients jointly influence post-fire habitat models in mixed-conifer forests of Yosemite National Park, USA. Fire 3, 54. https://doi.org/10.3390/fire3040054.

Taudière, A., Richard, F., Carcaillet, C., 2017. Review on fire effects on ectomycorrhizal symbiosis, an unachieved work for a scalding topic. For. Ecol. Manag. 391, 446–457. https://doi.org/10.1016/j.foreco.2017.02.043.

Team, Fire Behavior Assessment, 2022. FBAT 2022 Measurement Protocols. United States Department of Agriculture.

Vakili, E., Hoffman, C.M., Keane, R.E., Tinkham, W.T., Dickinson, Y., 2016. Spatial variability of surface fuels in treated and untreated ponderosa pine forests of the southern Rocky Mountains. Int. J. Wildland Fire 25, 1156–1168. https://doi.org/10.1071/WF16072.

Van Wagner, C., 1983. E. Fire behaviour in northern conifer forests and shrublands. In: Wein, Ross W., Maclean, David A. (Eds.), The Role of Fire in Northern Circumpolar Ecosystems. John Wiley & Sons, New York, NY, pp. 65–80.

van Wagtendonk, J.W., Moore, P.E., Yee, J.L., Lutz, J.A., 2020. The distribution of woody species in relation to climate and fire in Yosemite National Park, California, USA. Fire Ecol. 16, 22. https://doi.org/10.1186/s42408-020-00079-9.

Walters, W., Hyde, E.R., Berg-Lyons, D., Ackermann, G., Humphrey, G., Parada, A., et al., 2016. Improved bacterial 16S rRNA gene (V4 and V4-5) and fungal internal transcribed spacer marker gene primers for microbial community surveys. mSystems 1. https://doi.org/10.1128/msystems.00009-15.

Wang, T., Hamann, A., Spittlehouse, D., Carroll, C., 2016. Locally downscaled and spatially customizable climate data for historical and future periods for North America. PLoS One 11, e0156720. https://doi.org/10.1371/journal.pone.0156720.

Wasserman, T.N., Mueller, S.E., 2023. Climate influences on future fire severity: a synthesis of climate-fire interactions and impacts on fire regimes, high-severity fire, and forests in the western United States. Fire Ecol. 19, 43. https://doi.org/10.1186/s42408-023-00200-8.

Wasyliw, J., Karst, J., 2020. Shifts in ectomycorrhizal exploration types parallel leaf and fine root area with forest age. J. Ecol. 108, 2270–2282. https://doi.org/10.1111/1365-2745.13484.

Weber, M.G., Wagner, C.E.V., Hummel, M., 1987. Selected parameters of fire behavior and *Pinus banksiana* lamb. Regeneration in eastern Ontario. For. Chron. 63, 340–346. https://doi.org/10.3390/fire203004110.5558/tfc63340-5.

Weltzin, J.F., Keller, J.K., Bridgham, S.D., Pastor, J., Allen, P., Chen, J., 2005. Litter controls plant community composition in a northern fen. Oikos 110, 537–546. https://doi.org/10.1111/j.0030-1299.2005.13718.x.

White, T.J., Bruns, T., Lee, S., Taylor, J., 1990. Amplification and direct sequencing of fungal ribosomal RNA genes for phylogenetics. PCR protocols: a guide to methods and applications 18, 315–322.

Whitman, T., Whitman, E., Woolet, J., Flannigan, M.D., Thompson, D.K., Parisien, M.-A., 2019. Soil bacterial and fungal response to wildfires in the Canadian boreal forest across a burn severity gradient. Soil Biol. Biochem. 138, 107571. https://doi.org/10.1016/j.soilbio.2019.107571.

Whitman, T., Woolet, J., Sikora, M., Johnson, D.B., Whitman, E., 2022. Resilience in soil bacterial communities of the boreal forest from one to five years after wildfire across a severity gradient. Soil Biol. Biochem. 172, 108755. https://doi.org/10.1016/j.soilbio.2022.108755.

Whittaker, R.H., 1960. Vegetation of the Siskiyou mountains, Oregon and California. Ecol. Monogr. 30, 279–338.

Wickham, H., 2016. ggplot2: Elegant Graphics for Data Analysis. Springer International Publishing. https://doi.org/10.1007/978-3-319-24277-4_9.

Wilson Jr., R.A., 1985. Observations of extinction and marginal burning states in tree burning porous fuel beds. Combust. Sci. Technol. 44, 179–193. https://doi.org/10.1080/00102208508960302.

Yang, S., Limpens, J., Sterck, F.J., Sass-Klaassen, U., Cornelissen, J.H., Hefting, M., et al., 2021. Dead wood diversity promotes fungal diversity. Oikos 130, 2202–2216. https://doi.org/10.1111/oik.08388.

Yang, T., Tedersoo, L., Liu, X., Gao, G.-F., Dong, K., Adams, J.M., et al., 2022. Fungi stabilize multi-kingdom community in a high elevation timberline ecosystem. iMeta 1, e49. https://doi.org/10.1002/imt2.49.

Yaveroğlu, Ö.N., Malod-Dognin, N., Davis, D., Levnajic, Z., Janjic, V., Karapandza, R., et al., 2014. Revealing the hidden language of complex networks. Sci. Rep. 4, 4547. https://doi.org/10.1038/srep04547.

Ziegler, J.P., Hoffman, C.M., Mell, W., 2019. firebehavioR: an R package for fire behavior and danger analysis. Fire 2, 41. https://doi.org/10.3390/fire2030041.

Zosso, C.U., Ofiti, N.O.E., Torn, M.S., Wiesenberg, G.L.B., Schmidt, M.W.I., 2023. Rapid loss of complex polymers and pyrogenic carbon in subsoils under whole-soil warming. Nat. Geosci. 16, 344–348. https://doi.org/10.1038/s41561-023-01142-1.